Fermi National Accelerator Laboratory

FERMILAB-Pub-75/35-THY
April 1975

Consequences for Neutrino Production of M^0 Heavy Leptons

CARL H. ALBRIGHT
Fermi National Accelerator Laboratory, Batavia, Illinois 60510
and
Northern Illinois University*, DeKalb, Illinois 60115

ABSTRACT

Monte Carlo calculations are presented for neutrino production of neutral heavy leptons which rapidly decay into dimuons and neutrinos, neutrinos only, muons and hadrons, and neutrinos and hadrons. For a mass of 4-5 GeV, the relative cross sections, branching ratios, and observed energy, x, y and W distributions are all presently compatible with the data on dimuon production and anomalous effects recently reported.

---

*Permanent address.

Operated by Universities Research Association Inc. under contract with the Energy Research and Development Administration

FERMILAB-Pub-75/35-THY

Consequences for Neutrino Production of M^0 Heavy Leptons

CARL H. ALBRIGHT
Fermi National Accelerator Laboratory, Batavia, Illinois 60510
and
Northern Illinois University, DeKalb, Illinois 60115

ADDENDUM

Since this paper was written, preliminary results from a recent higher energy neutrino run have been presented at the Washington APS Meeting by the Harvard-Penn-Wisconsin-Fermilab group. Thirty-two $\mu^+ - \mu^-$ events were reported in the new sample along with 4 events at the $\mu^- - \mu^-$ variety. Whether the latter are just accidentals resulting from π or K decays is unclear. Only two of the 32 $\mu^+ - \mu^-$ events have a dimuon mass $M_{\mu\mu} > 5$ GeV; however, the observed μ^- energy distribution appears to be slightly broader than expected while the μ^+ energy distribution is slightly narrower than expected if the $\mu^+ - \mu^-$ signal were due solely to heavy lepton production and decay.

I. INTRODUCTION

In a previous investigation,[1] the author in collaboration with C. Jarlskog and L. Wolfenstein studied neutrino production of M^+ and E^+ heavy leptons. A striking signal for M^+ production is the observation of "wrong sign" muons arising from the $M^+ \to \nu_\mu \mu^+ \nu_\mu$ decay mode and resulting in the apparent violation of lepton conservation in the transition. The Cal Tech neutrino group[2] has subsequently placed a lower bound of 8.4 GeV/c^2 on the mass of the M^+ by their failure to observe more than 8 μ^+ events which occurred at a level consistent with the $\bar{\nu}_\mu$ background in their ν_μ dichromatic beam.

In this paper, we wish to extend our analysis to neutrino production of M^0 heavy leptons.[3] This is prompted by the recent observation of 14 dimuon events by the Harvard-Penn-Wisconsin-Fermilab neutrino group[4] and of some 20 dimuon events by the Cal Tech-Fermilab neutrino group.[5]

The general features of these dimuon events reported which we wish to single out are the following:[6]

1) All muon pairs for which the charges have been determined are of the μ^+-μ^- variety;

2) The event rate[5] is a factor of $\sim$ 10 greater at E = 150 GeV than at 50 GeV;

3) All dimuon events have an invariant mu pair mass

$M_{\mu\mu} \lesssim 4$ GeV/c^2 with the exception of two events (one[5] with $M_{\mu\mu} = 5.4$ GeV and one[4] with $M_{\mu\mu} = 7.1$ GeV);

4) For most events $E_{\mu^-} > E_{\mu^+}$;

5) For all events $x_{obs} = q'^2/2\nu' \lesssim 0.2$ determined for the μ^- relative to the incident ν_μ;

6) The distribution for $y_{obs} = E_{had}/(E_{had} + E_{\mu^-} + E_{\mu^+})$ is rather broad but appears to be centered at a higher value in the Cal Tech run than in the HPWF run;

7) The observed W distribution of the system recoiling against the negative muon has $W_{min} \geq 4$ GeV in the HPWF run and $W > 9$ GeV in the Cal Tech run but for one event.

These seven features are quite striking and suggest some new particle production. We wish to pursue here the possibility the dimuon events are at least partly due to inclusive M^0 production

$$\nu_\mu + N \rightarrow M^0 + X \tag{1.1}$$

and decay via the leptonic mode

$$M^0 \rightarrow \mu^- + \mu^+ + \nu_\mu \quad . \tag{1.2a}$$

Other decay modes such as

$$M^0 \rightarrow \mu^- + x \tag{1.2b}$$

$$M^0 \rightarrow \nu_\mu + x \tag{1.2c}$$

and

$$M^0 \rightarrow \nu_\mu + \bar{\nu}_\ell + \nu_\ell \tag{1.2d}$$

will appear to be ordinary charged-current or neutral-current events. However, for all three types of decays, the x, y and W distributions are characteristically different from the distributions associated with the background processes as will be illustrated. In fact, the W distributions obtained are very much like the anomalous W distributions published recently by the HPWF neutrino group.[7]

Other competing mechanisms such as charm particle production

$$\nu_\mu + N \rightarrow \mu^- + C + X \tag{1.3}$$

followed by charmed particle decay

$$C \rightarrow x + \ell^+ + \nu_\ell \tag{1.4}$$

or

$$C \rightarrow x$$

can also lead to dimuon events, etc. So it will eventually be necessary to examine each mechanism in detail in order to single out the one effect (or several) which may be responsible for the anomalous signals.

In the analysis to be presented, we find that the relative event rates at 50 and 150 GeV and the slope of the invariant dimuon mass spectrum (points 2 and 3 above) impose a heavy lepton mass in the range 4-5 GeV. Helicity arguments suggest that we consider primarily a V-A form for the production and decay vertices in (1.1) and (1.2) in order to comprehend point 4. In Sec. II we present the basic formulas, while in Secs. III, IV and V we give the results of our Monte Carlo calculations for the dileptonic, single muon and muonless decay channels of the heavy M^0. Results for both neutrino- and antineutrino-induced reactions are illustrated, for the apparent differences may help considerably in

discriminating heavy lepton effects from charm particle effects which tend to favor diffractive production.[8]

II. PRODUCTION AND DECAY MECHANISMS

We begin by noting that most dimuon events observed to date have[4,5] $E_{\mu^-} > E_{\mu^+}$ and are probably produced by neutrinos rather than antineutrinos.[5] Hence we shall assume a V-A structure for the neutral current $\nu_\mu - M^0$ production vertex as well as a V-A interaction for the charged (and neutral) current decay. This assumption tends to produce the M^0 left handed with the subsequent μ^- emitted primarily in the forward hemisphere, while the μ^+ is emitted in the backward hemisphere in the M^0 rest frame. Any V + A admixture at the lepton vertices, for example, will weaken this effect and reduce the $E_{\mu^-} - E_{\mu^+}$ asymmetry.

For the hadronic vertex, we also assume a V-A form for simplicity.[9] The production process is then very comparable to the neutrino production of M^+ treated earlier.[1] We simply summarize the basic formulas and refer the reader to papers (I) and (II). In the scaling region, the differential cross section for (1.1) and its antineutrino counterpart is given by[10]

$$\frac{d^2\sigma^{\nu,\bar{\nu}}}{dxdy} = \frac{G^2 ME}{\pi}\left\{\left(xy + \frac{m^2}{2ME}\right)y F_1 + \left[(1-y) - \left(\frac{M}{2E}xy + \frac{m^2}{4E^2}\right)\right]F_2 \right.$$
$$\left. \mp \left[xy\left(1-\tfrac{1}{2}y\right) - \frac{m^2}{4ME}y\right]F_3 + \frac{m^2}{M^2}\left[\left(\frac{M}{2E}xy + \frac{m^2}{4E^2}\right)F_4 - \frac{M}{2E}F_5\right]\right\} \quad (2.1)$$

in terms of the scaling variables $x = q^2/2\nu$ and $y = \nu/ME$, the heavy lepton mass m, the nucleon mass M, and the structure functions F_i which are functions only of x. The Callan-Gross relation

$$2xF_1 = F_2 \tag{2.2a}$$

and the relation[11]

$$-xF_3 = F_2 \tag{2.2b}$$

further restrict F_4 and F_5 to

$$F_4 = 0, \quad xF_5 = F_2 \ . \tag{2.2c}$$

For our numerical work, we take

$$\begin{aligned} F_2^{\nu N \to M^0 X} &\approx F_2^{\nu N \to \mu^- X} \\ &= 3.06\,(1-x)^3 - 6.08(1-x)^4 + 28.21\,(1-x)^5 \\ &\quad - 41.40\,(1-x)^6 + 17.28\,(1-x)^7 \end{aligned} \tag{2.3}$$

as in (I) and (II). These expressions lead directly to the energy-dependent cross sections shown in Fig. 1. For a mass of 4-5 GeV for the heavy lepton, the ν and $\bar{\nu}$ cross sections at 150 GeV are roughly 10 times those at 50 GeV.

The heavy lepton is produced partially polarized. In its rest frame the polarization vector is given by

$$\begin{aligned} (\vec{P})_{\nu,\bar{\nu}} = \pm \frac{G^2}{2\pi} m \Bigg\{ \left[2yF_1 - \frac{M}{E} F_2 \mp F_3 - \frac{m^2}{ME} F_4 + (1-y)F_5 \right] \vec{k} \\ + \left[2F_2 - (xy + \frac{m^2}{2ME})(\pm F_3 + F_5) \right] \vec{p} \Bigg\} \Big/ \frac{d^2\sigma^{\nu,\bar{\nu}}}{dxdy} \ , \end{aligned} \tag{2.4}$$

in terms of $\vec{k}$ and $\vec{p}$, the momenta of the neutrino and incident nucleon in that frame.

Turning to the heavy lepton decay modes, we first examine the dimuon mode (1.2a). With a V-A form for the charged (and neutral) current interaction, the spectrum of the emitted lepton (μ^- or ν_μ) in the rest frame of the decaying $M^0 \to \mu^- \mu^+ \nu_\mu$ is given by

$$\frac{dw_{-,0}}{d\epsilon d\Omega} = \frac{G^2}{8(2\pi)^4} m^5 \epsilon^2 \left(1 - \frac{2}{3}\epsilon\right)(1 + \alpha_{-,0} |\vec{P}| \cos\theta) \qquad (2.5a)$$

where $\vec{P}$ is the polarization vector in (2.4), ϵ is the ratio of the energy carried off by the decay lepton to its maximum value, and α is the asymmetry parameter which is equal to

$$\alpha_- = \alpha_0 = (1-2\epsilon)/(3-2\epsilon) \ . \qquad (2.5b)$$

The spectrum of the emitted μ^+, on the other hand, is given by

$$\frac{dw_+}{d\epsilon d\Omega} = \frac{G^2}{4(2\pi)^4} m^5 \epsilon^2 (1-\epsilon)(1+\alpha_+ |\vec{P}| \cos\theta) \qquad (2.6)$$

with $\alpha_+ = +1$.

The invariant mass $M_{\mu\mu}$ of the dimuon pair is simply related to the energy taken by the outgoing neutrino in the M^0 rest frame by $M_{\mu\mu}^2 = m^2(1-\epsilon_0)$. Hence the probability spectrum for $z^2 = (M_{\mu\mu}/m)^2$ is just

$$\frac{dP}{dz^2} = 2(1-z^2)^2(1+2z^2) \qquad (2.7a)$$

while that for $z = M_{\mu\mu}/m$ is

$$\frac{dP}{dz} = 4z(1-z^2)^2(1+2z^2) \ . \qquad (2.7b)$$

Both distributions reflect the outgoing neutrino energy spectrum, but the invariant mass distribution (2.7b) is considerably distorted by the transformation.

The latter is plotted in Fig. 2. The falloff near $M_{\mu\mu} = m$ reflects the low energy behavior of the outgoing neutrino in the M^0 rest frame which is insensitive to the value of the ρ-parameter for the decay. A ρ-parameter different from 0.75 for our choice of V-A current interaction will only seriously affect the low z-behavior. Since all but two of the measured dimuon events have $M_{\mu\mu} \lesssim 4$ GeV, we shall now focus our attention on a heavy lepton mass $m = 4$ GeV. Those 2 events must then result from a different phenomenon in our picture.[12]

Consider now the semileptonic decays $M^0 \to \mu^- + x$ and $M^0 \to \nu_\mu + x$ where the hadrons are unobserved except for their total energy. As in (I), we express the hadronic tensor appearing in these decay modes as

$$\begin{aligned} W_{\mu\nu} &= \tfrac{1}{2}(2\pi)^4 \sum_F \langle 0 | J_\mu^* | F \rangle \langle F | J_\nu | 0 \rangle \delta(q - p_F) \\ &= (q^2 \delta_{\mu\nu} - q_\mu q_\nu) W_1(q^2) - q_\mu q_\nu W_2(q^2) \end{aligned} \tag{2.8}$$

in terms of two structure functions which depend only on $q^2 = -s$, the invariant mass squared of the outgoing hadrons. The decay spectrum in the M^0 rest frame for the outgoing lepton (μ^- or ν_μ) can then be expressed as

$$\begin{aligned} \frac{dw}{d\epsilon\, d\Omega} = \frac{G^2}{8(2\pi)^3} m^5 \epsilon^2 \Big\{ &(3-2\epsilon)\left[1 + \alpha_1 |\vec{P}| \cos\theta\right] W_1(-m^2(1-\epsilon)) \\ &+ \left[1 + \alpha_2 |\vec{P}| \cos\theta\right] W_2(-m^2(1-\epsilon)) \end{aligned} \tag{2.9}$$

where $\vec{P}$ is the polarization vector given in (2.4) and the asymmetry

parameters are found to be $\alpha_1 = \alpha_0 = \alpha_-$ of (2.5b) and $\alpha_2 = -1$. Following the argument presented in (I), we make use of the SPEAR data on e^+e^- annihilation and set[13]

$$W_1(-s) = \frac{1}{4\pi}\left(-0.4 + 1.2\,\frac{\sqrt{s}}{M}\right)$$

$$W_2(-s) = 0 \quad . \tag{2.10}$$

We now have all the ingredients necessary to make Monte Carlo calculations for the chain reations

$$\nu_\mu + N \rightarrow M^0 + X$$

$$\rightarrow \mu^- \mu^+ \nu_\mu \tag{2.11a}$$

$$\rightarrow \nu_\mu \bar{\nu}_\ell \nu_\ell \tag{2.11b}$$

$$\rightarrow \mu^- X \tag{2.11c}$$

$$\rightarrow \nu_\mu X \tag{2.11d}$$

For this purpose, we randomly select 4000 points in the q^2-ν plane corresponding to the production process (1.1) and map each point into 1000 points in the effective q'^2- ν' plane for the various chain processes in (2.11). We refer the reader to our earlier publications for details.[1,3]

Note that we can obtain equivalent results for the antineutrino chain reactions

$$\bar{\nu}_\mu + N \rightarrow \bar{M}^0 + X$$

$$\rightarrow \mu^+ \mu^- \bar{\nu}_\mu \tag{2.12a}$$

$$\rightarrow \bar{\nu}_\mu \nu_\ell \bar{\nu}_\ell \tag{2.12b}$$

$$\rightarrow \mu^+ X \tag{2.12c}$$

$$\rightarrow \bar{\nu}_\mu X \tag{2.12d}$$

simply by replacing $F_3(x)$ by $-F_3(x)$.

III. DIMUON PRODUCTION

In Figs. 3(a), (b) and (c) are shown the statistical fractions of the total energy carried out by the muons and hadrons in the chain process (2.11a) for incident neutrino energies of E = 50, 150 and 250 GeV. For all three energies and as a result of our V-A lepton current assumptions the μ^- tends to be emitted with more energy than the μ^+. The missing neutrino has the same probability distribution as the μ^-. The hadrons take proportionally more energy as E increases from 50 to 250 GeV.

The $y_{obs} = E_{had}/(E_{had} + E_{\mu^-} + E_{\mu^+})$ distributions at energies E = 50, 100, 150 and 250 GeV are illustrated in Fig. 4. As E increases from 50 GeV to 250 GeV, there is a dramatic shift in the y_{obs} distribution toward higher values. This reflects the features stated in the above paragraph. In the HPWF run with a single focussing horn, a broad band neutrino beam was obtained with a flux spectrum which peaked in the neighborhood of 30 GeV and fell through several orders of magnitude as E approached 100 GeV. In the CalTech run with a dichromatic neutrino beam peaked at 50 and 150 GeV, nearly all the dimuon events resulted from the higher energy K neutrino flux. Hence Fig. 4 is quite compatible with point 6 of the Introduction.

Figure 5 illustrates that the apparent $x_{obs} = q'^2/2\nu'$ distribution is peaked at small values of x_{obs} for all energies, with the peaking becoming even more pronounced at the higher energies. The solid curves refer to x_{obs} as measured by the outgoing μ^-, while the dashed

curves refer to x_{obs} for the μ^+. The μ^+ x_{obs} distributions are even more sharply peaked than the μ^- ones.

The apparent $W/\sqrt{s}$ distributions are shown in Fig. 6 with the same convention regarding solid and dashed curves as in Fig. 5. The E = 250 GeV curves fall nearly on top of the E = 150 GeV ones and are not plotted. The W distributions peak at large values of $W/\sqrt{s}$ for all energies and, in fact, are negligibly small for $W/\sqrt{s} < 0.5$. At E = 50 GeV, $W/\sqrt{s} = 0.5$ corresponds to W = 4.9 GeV while at E = 150 GeV, it corresponds to W = 8.4 GeV.

The corresponding distributions for the antineutrino chain reaction (2.12a) are given in Figs. 7-10. In this process the μ^+ tends to take more energy than the μ^-. The x_{obs} and $W/\sqrt{s}$ distributions are very similar to those for the neutrino process, but the y_{obs} distributions are very different for the two processes. From Fig. 8 for the anti-neutrino process we observe that y_{obs} is peaked at very low values for E = 50 GeV and shifts somewhat to higher y_{obs} values as E increases to 150 GeV, but the shift is not nearly so dramatic as in Fig. 4 for the neutrino process.

This feature reflects our assumption of V-A neutral current coupling at the hadronic production vertex. If we had assumed simply V or A coupling at the neutral-current hadronic vertex, the ν and $\bar{\nu}$ y_{obs} distributions would be identical. They are shown in Fig. 11 for comparison.

IV. SINGLE MUON PRODUCTION

We now turn our attention to the single muon production chain

distributions for both the neutrino-induced (solid curves) and antineutrino-induced (dashed curves) reactions.[14] The curves are peaked at high values of y_{eff}, even more so for the neutrino reaction and at the higher energies. In contrast, the simple results expected for the ordinary reactions without M^0 production

$$\nu_\mu + N \to \mu^- + X \tag{4.1}$$

$$\bar{\nu}_\mu + N \to \mu^+ + X \tag{4.2}$$

are shown as dotted and double-dotted curves respectively.

The $W/\sqrt{s}$ curves for the chain reactions are plotted in Figs. 13 and 14 respectively, where the results expected for the ordinary inclusive reactions are also given. The latter curves follow from the expression

$$\frac{1}{\sigma}\frac{d\sigma^{\nu,\bar{\nu}}}{d\eta} = \frac{2\eta\int_0^{1-\eta^2} dx\,\frac{1}{1-x}\left[1,\left(1-\frac{\eta^2}{1-x}\right)^2\right]F_2(x)}{\left[1,\frac{1}{3}\right]\int_0^1 dx\,F_2(x)} \tag{4.3}$$

with $\eta = W/\sqrt{2ME} \sim W/\sqrt{s}$. The peaking at high values of $W/\sqrt{s}$ occurs well out on the tail of the background curve only for the antineutrino chain reaction.

V. MUONLESS PROCESSES

The muonless reactions (2.11b, d) and (2.12b, d) resulting from M^0 decay arise from two different decay modes. In the case of $M^0 \to \nu_\mu + x$ and its antilepton counterpart, the distributions for

$$y_{eff} = E_{had}/E = (E_X + E_x)/E \tag{5.1}$$

are just the y_{eff} curves shown in Fig. 12 for the (2.11c) and (2.12c) reactions.

For the all-neutrino decay mode $M^0 \to \nu_\mu \bar{\nu}_\ell \nu_\ell$ the

$$y_{eff} = E_X/E \tag{5.2}$$

distributions are drawn in Figs. 15 and 16. The absence of a peaking at high y in the (5.2) curves indicates that the peaking in the (5.1) curves results primarily from the hadrons emitted in the decay of the heavy lepton.

VI. GENERAL OBSERVATIONS

We conclude our study of neutrino production of neutral heavy leptons by noting that all numerical results obtained for the dileptonic reaction are consistent with the seven experimental features elaborated in the Introduction; moreover, the anomalous W distributions for the single muon events are compatible with those reported by the HPWF group.[7]

Both the relative M^0 production cross sections at 50 and 150 GeV being in the ratio 1:10 and the invariant dimuon mass bound, $M_{\mu\mu} \lesssim 4$ GeV, are consistent with a heavy lepton mass of 4-5 GeV. A mass of 7 GeV ,on the other hand, implies $\sigma(50\ \text{GeV}) : \sigma(150) \sim 1:200$

which appears inconsistent with point 2 as well as poorly describing the invariant $M_{\mu\mu}$ mass spectrum reported.

The energy distributions of the μ^-, μ^+ and the hadrons are qualitatively in good agreement with those obser ved experimentally for the dimuon events. The x_{obs} distributions are peaked at small x while the W distributions are peaked at large $W/\sqrt{s}$, also in good agreement with the present data from both neutrino groups.

The $y_{obs} = E_{had}/(E_{had} + E_{\mu^-} + E_{\mu^+})$ distributions also appear to be in good qualitative agreement with the data. If it is borne out experimentally that the y_{obs} curves for the neutrino reaction (2.11a) shift dramatically toward higher y values as E increases while those for the antineutrino reaction (2.12a) remain peaked at the lower y values, this will confirm a sizable V-A interference term for the neutral-current hadronic production vertex. This result would also favor the M^0 process over charmed particle production (1.3) and decay (1.4). The latter effect is expected to be small[15] except for diffractive production of charm.[8] Such diffractive processes treat neutrino and antineutrino dimuon production equally, so the cross sections and y_{obs} distributions should be identical.

Concerning the single muon processes, we note general qualitative agreement there too. If $\bar{M}^0$ s are produced with sufficiently large cross sections at the higher energies, and if the branching ratio for the decay mode $\bar{M}^0 \rightarrow \mu^+ + x$ is reasonably large, the y distribution

for $\bar{\nu} \to \mu^+$ will be filled in considerably at high y. The corresponding distortion of the flat y distribution for $\nu \to \mu^-$ will not be as dramatic. Likewise, the peaking in the W distribution for the antineutrino process which occurs well out on the tail of the background distribution will persist while that for the neutrino process will tend to be covered up. The data of Ref. 7 can be understood in this fashion.

To assess the relative importance of the anomalous effects arising from M^0 decay via a semileptonic mode vs. that for the leptonic modes requires knowledge of the types and strengths of the neutral-current and charged-current couplings. These will vary from one gauge model to another. Allowing some speculation, we note that previous estimates[16] by Jarlskog, Tjia and the author for the branching ratio for the $M^0 \to \mu^- + x$ mode place it in the neighborhood of 50 percent for most gauge models, while that for the $M^0 \to \mu^- \mu^+ \nu_\mu$ mode can range from $\sim$ 1-20 percent. Hence estimates for the anomalous single muon to dimuon signals range from 2.5 to 50:1. We expect the neutral-current coupling constants in the production process are at most equal to those for the charged-current processes. A glance at Fig. 1 then reveals that with an M^0 mass of 4 GeV, the inclusive cross section for M^0 production relative to the ordinary process (4.1) is at most a factor of 1:4 at E = 100 GeV. Hence the anomalous single muon events should be limited to at most 12 percent of the background signal, while the dimuon events should be limited to 0.25-5 percent of the $\nu \to \mu^-$

signal. In fact, the relative experimental rates appear to be 14 percent and 1 percent respectively. Again the M^0 interpretation of the dimuon events and anomalous signals appears to be a plausible one which cannot be ruled out at this stage.

The critical test of this model will come when higher (and lower) energy data are obtained and analyzed. If the dimuon mass spectrum remains bounded by $M_{\mu\mu} < 4$-5 GeV and of a shape similar to that of Fig. 2, heavy M^0 production and decay is a viable explanation. If it turns out that a fair fraction of the dimuon events have $M_{\mu\mu} > 4$-5 GeV, the charm mechanism is the more likely explanation. It may happen, however, that most events appear to be confined below 4-5 GeV while only a relatively small background ($\sim$ 10-20 percent) of them appear out on the tail. This would possibly suggest that both heavy lepton and charm mechanisms are playing important roles.

NOTE ADDED

Since this paper was written, preliminary results from a recent higher energy neutrino run have been presented at the Washington APS Meeting by the Harvard-Penn-Wisconsin-Fermilab group. Thirty-two $\mu^+ - \mu^-$ events were reported in the new sample along with 4 events of the $\mu^- - \mu^-$ variety. Whether the latter are just accidentals resulting from π or K decays is unclear. Only two of the 32 $\mu^+ - \mu^-$ events have a dimuon mass $M_{\mu\mu} > 5$ GeV; however, the observed μ^- energy distribution appears to be slightly broader than expected while the μ^+ energy distribution is slightly narrower than expected if the $\mu^+ - \mu^-$ signal were due solely to heavy lepton production and decay.

ACKNOWLEDGMENTS

The author wishes to acknowledge Professor J. J. Sakurai for spirited discussions which led to this work. He thanks the Fermilab Theory Group for its kind hospitality and generous support for the Monte Carlo calculations carried out on the Argonne IBM 370-195 computer.

While our work was in progress, the author received a manuscript from Drs. L. N. Chang, E. Derman and J. N. Ng dealing with the same subject. We thank these authors for sending their paper to us and for pointing out a plotting error in the original version of Fig. 2.

FOOTNOTES AND REFERENCES

[1] C. H. Albright and C. Jarlskog, Nucl. Phys. B84, 467 (1975); C. H. Albright, C. Jarlskog, and L. Wolfenstein, Nucl. Phys. B84, 493 (1975). These papers are referred to as (I) and (II) respectively.

[2] B. C. Barish, et al., Phys. Rev. Lett. 32, 1387 (1974).

[3] The author first analyzed heavy lepton production and decay by Monte Carlo methods for a neutral heavy lepton decaying into the single channel $\mu^- \pi^+$; cf. C. H. Albright, Phys. Rev. Lett. 28, 1150 (1972); Phys. Rev. D7, 63 (1973).

[4] A. Benvenuti et al., Phys. Rev. Lett. 34, 419 (1975).

[5] B. C. Barish et al., CALT-68-495, paper presented at the Colloque International Physique du Neutrino a Haute Energie, Ecole Polytechnique, Paris, France, March 1975.

[6] We refer the reader to Refs. 4 and 5 for details. Since the data are preliminary and will be superceded shortly by new data with considerably more statistics, we omit detailed comparisons at this time.

[7] A. Benvenuti et al., Phys. Rev. Lett. 34, 597 (1975).

[8] B. A. Arbuzov, J. J. Gershtein, V. V. Lapin, V. N. Folomeshkin, Serpukhov preprint, IFVE-75-25.

[9]This form of the neutral current is suggested in gauge models where the current coupling ν_μ and M^0 transforms like a U^+-spin operator. In Sec. III, we make a brief reference to the case where no V-A interference occurs.

[10]We use the same Fermi coupling constant identified with the charged current for convenience.

[11]This is approximately true for the charged-current reactions.

[12]For example, they could result from prompt π decays or the charm mechanism (1.3) and (1.4). The normalized distributions for a heavy lepton mass of 5 GeV are only slightly different from those given for m = 4 GeV in Figs. 3-16.

[13]This is a fair approximation to the SPEAR data up to $s = 16\ \text{GeV}^2$. A. Litke et al., Phys. Rev. Lett. 30, 1189 (1973); J.-E. Augustin, Phys. Rev. Lett. 34, 764 (1975).

[14]We have not plotted the x_{obs} distributions since they are so similar to those for dimuon production.

[15]C. H. Albright, Nucl. Phys. B75, 539 (1974).

[16]C. H. Albright, C. Jarlskog and M. O. Tjia, Nucl. Phys. B86, 535 (1975).

FIGURE CAPTIONS

Fig. 1 Inclusive cross sections for neutrino (solid curves) and antineutrino (dashed curves) production of M^0 heavy leptons off an isoscalar nucleon target.

Fig. 2 Invariant dimuon mass distributions predicted for $M^0 \to \mu^- \mu^+ \nu_\mu$ with V-A couplings.

Fig. 3 Fraction of the total energy shared by the outgoing μ^- (or ν_μ), μ^+, X = hadrons, and $\mu^- + \mu^+ + X$ at E = (a) 50 GeV, (b) 150 GeV, (c) 250 GeV in the neutrino production process.

Fig. 4 $y_{obs} = E_{had}/(E_{had} + E_{\mu^-} + E_{\mu^+})$ distributions for neutrino production of dimuons at E = 50, 100, 150 and 250 GeV.

Fig. 5 x_{obs} distributions for dimuon production at E = 50 and 150 GeV where the momentum transfer and energy transfer are calculated for the μ^- (solid curves) and μ^+ (dashed curves) with respect to the incident ν_μ.

Fig. 6 Apparent $W/\sqrt{s}$ distributions at E = 50 and 150 GeV calculated for the μ^- (solid curves) and μ^+ (dashed curves) with respect to the incident ν_μ.

Fig. 7 Fraction of the total energy shared by the outgoing μ^+ (or $\bar{\nu}_\mu$), μ^-, X = hadrons, and $\mu^+ + \mu^- + X$ at

E = (a) 50 GeV, (b) 150 GeV in the antineutrino production process.

Fig. 8 $y_{obs} = E_{had}/(E_{had} + E_{\mu^+} + E_{\mu^-})$ distributions for antineutrino production of dimuons at E = 50, 100 and 150 GeV.

Fig. 9 x_{obs} distributions for dimuon production by antineutrinos at E = 50 and 150 GeV where the momentum transfer and energy transfer are calculated for the μ^+ (solid curves) and μ^- (dashed curves) with respect to the incident $\bar{\nu}_\mu$.

Fig. 10 Apparent $W/\sqrt{s}$ distributions at E = 50 and 150 GeV calculated for the μ^+ (solid curves) and μ^- (dashed curves) with respect to the incident $\bar{\nu}_\mu$.

Fig. 11 y_{obs} distributions for neutrino or antineutrino production of dimuons with no V, A interference at the hadronic production vertex.

Fig. 12 $y_{eff} = E_{had}/E$ for neutrino (solid curves) and antineutrino (dashed curves) production of single muons via the heavy lepton chain reactions. The background curves for $\nu \to \mu^-$ and $\bar{\nu} \to \mu^+$ without heavy lepton production are indicated by dotted and double dotted curves respectively.

Fig. 13 Apparent $W/\sqrt{s}$ distributions for neutrino production of single muons through the M^0 chain reaction. The dashed curve indicates the expected background reactions.

Fig. 14 Same as for Fig. 13 but for antineutrino production of single muons.

Fig. 15 $y_{eff} = E_X/E$ distributions for neutrino production of muonless events through the M^0 process (2.11b).

Fig. 16 $y_{eff} = E_X/E$ distributions for antineutrino production of muonless events through (2.12b).

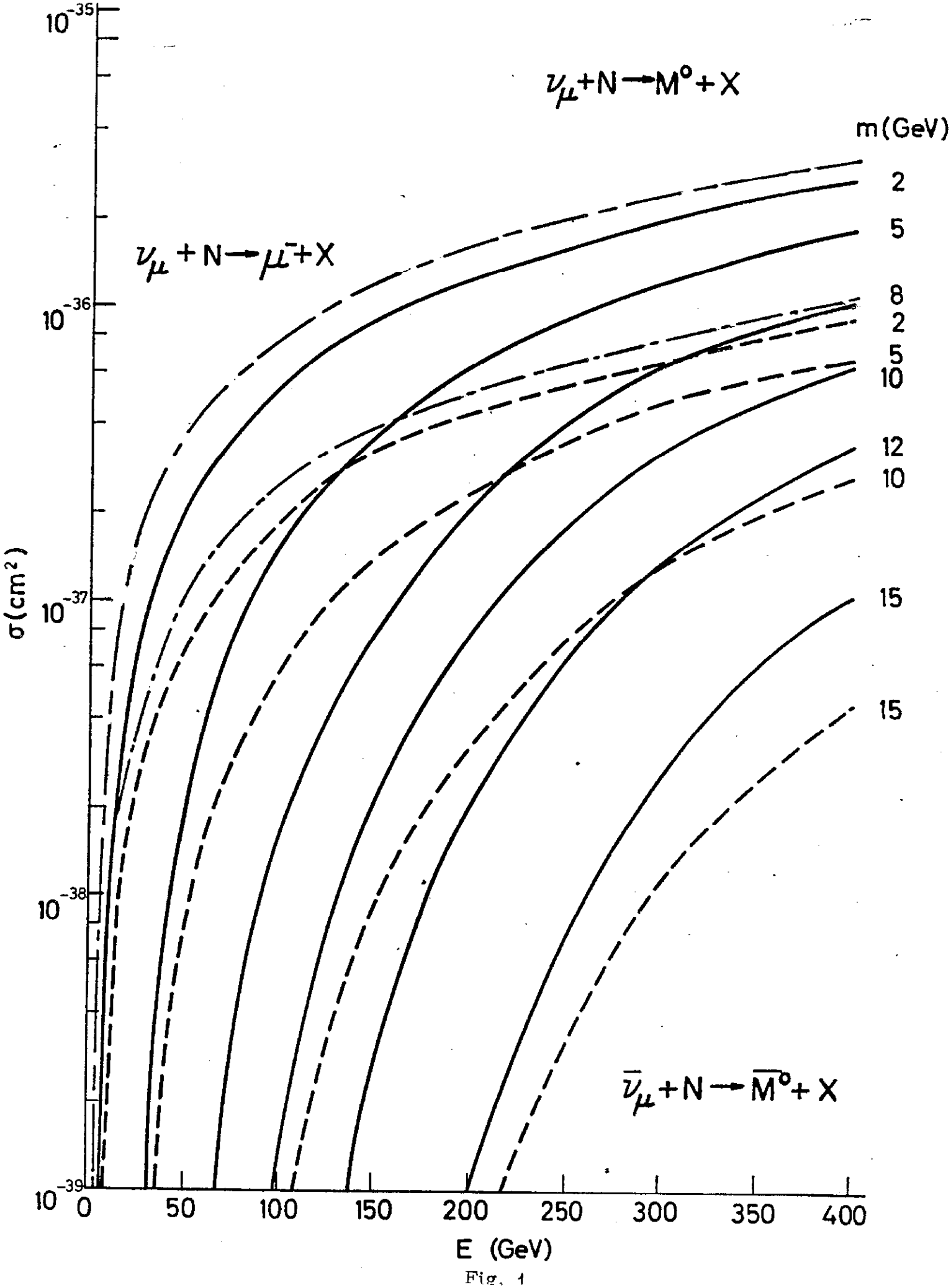
$\nu_\mu + N \rightarrow M^0 + X$
$\nu_\mu + N \rightarrow \mu^- + X$
$\bar{\nu}_\mu + N \rightarrow \bar{M}^0 + X$
m(GeV)
2
5
8
2
5
10
12
10
15
15
$\sigma(cm^2)$
10^{-35}
10^{-36}
10^{-37}
10^{-38}
10^{-39}
0
50
100
150
200
250
300
350
400
E (GeV)

Fig. 1

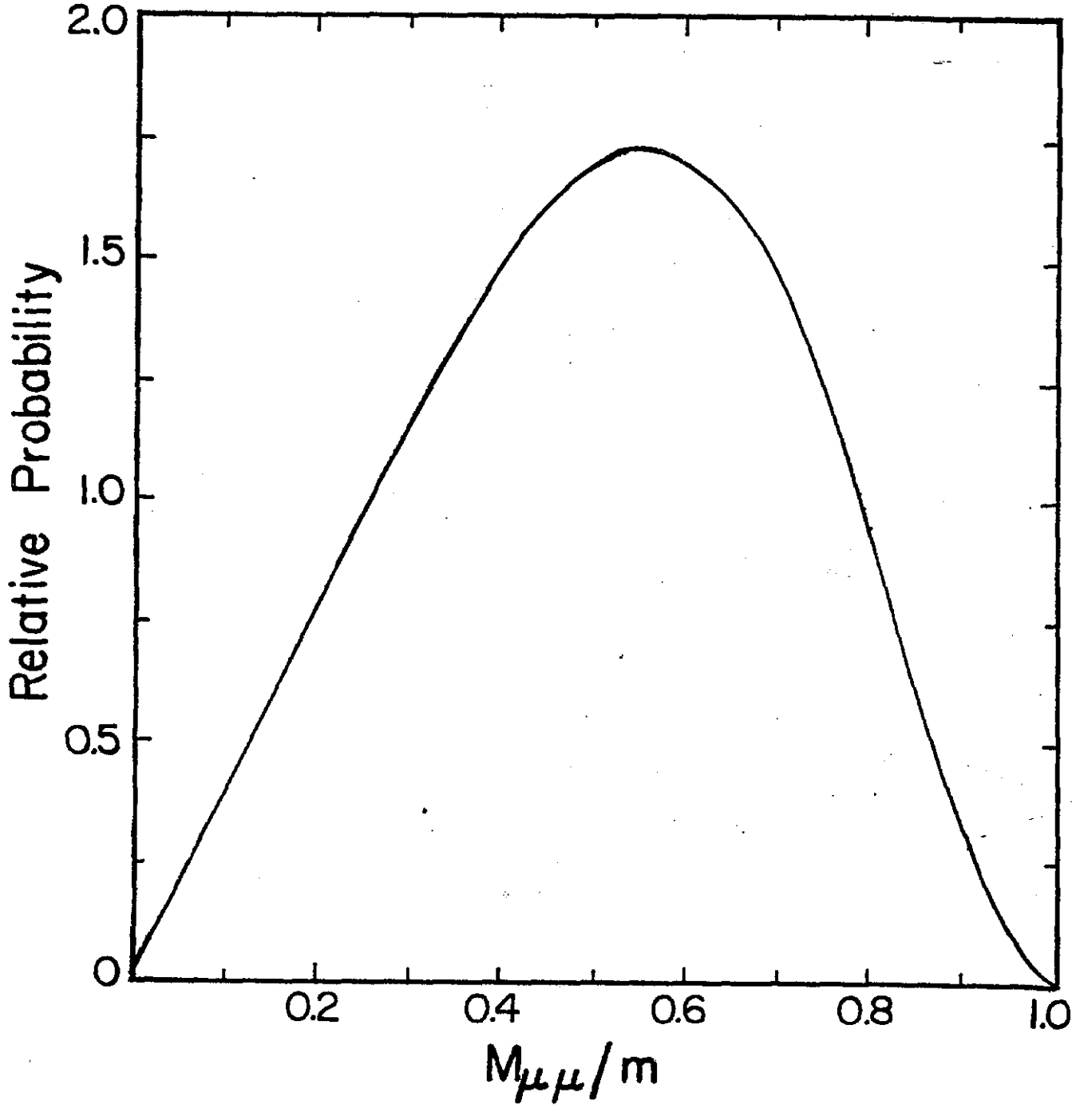

Fig. 2

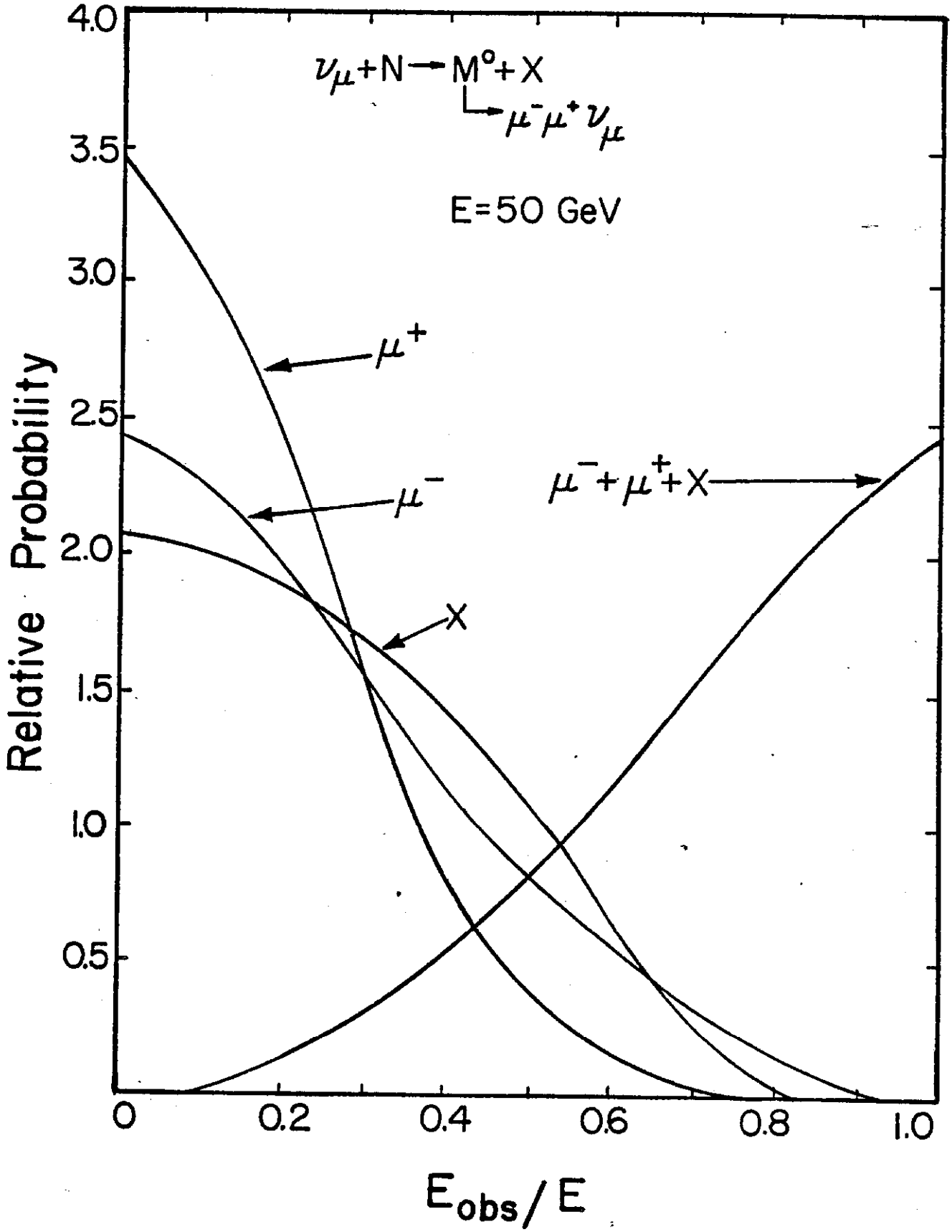
$\nu_\mu + N \rightarrow M^0 + X$
$\hookrightarrow \mu^- \mu^+ \nu_\mu$
E=50 GeV
μ^+
μ^-
$\mu^- + \mu^+ + X$
X
Relative Probability
4.0
3.5
3.0
2.5
2.0
1.5
1.0
0.5
0
0.2
0.4
0.6
0.8
1.0
E_{obs}/E

Fig. 3(a)

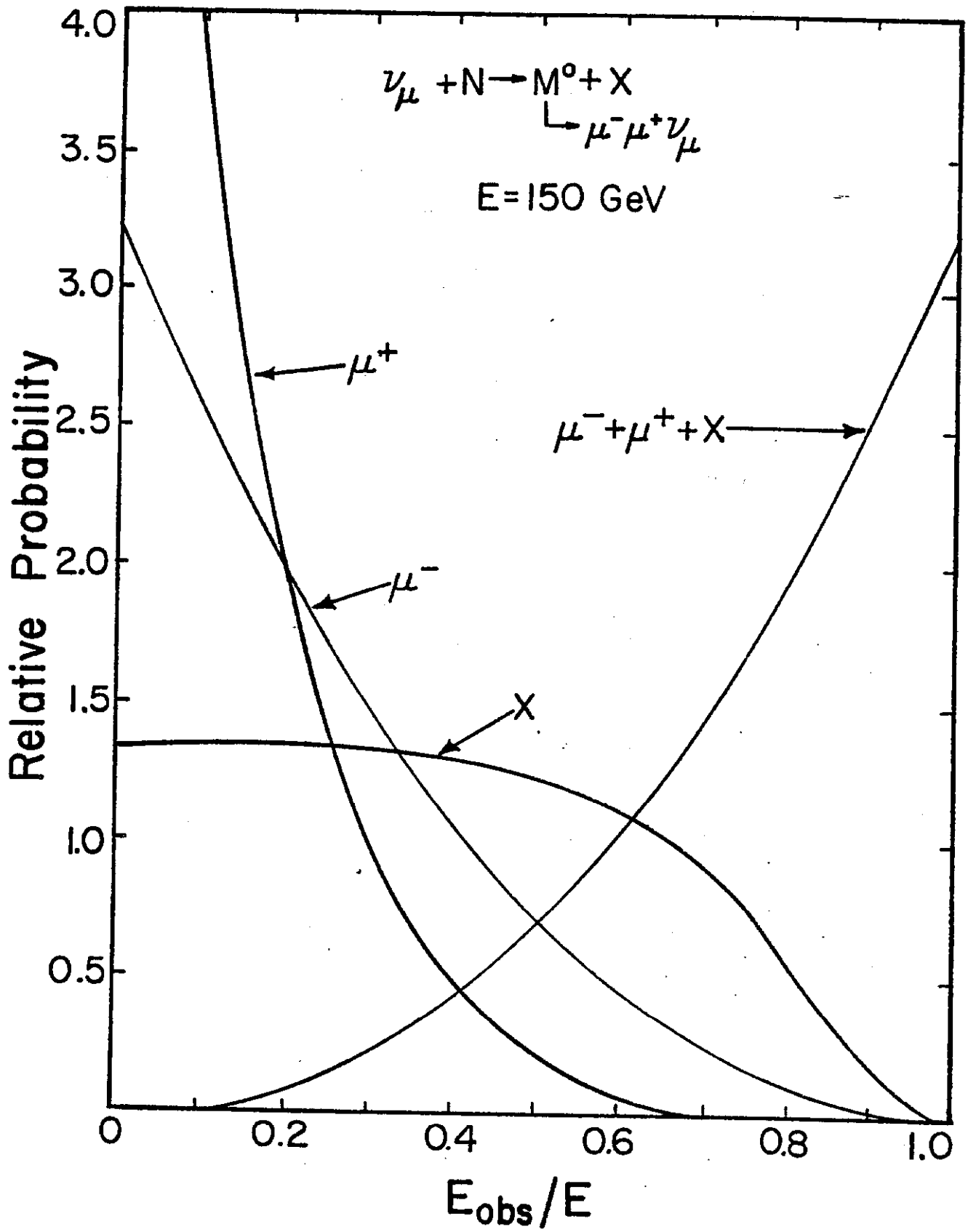
$\nu_\mu + N \rightarrow M^o + X$
$\hookrightarrow \mu^-\mu^+\nu_\mu$
E=150 GeV
μ^+
$\mu^- + \mu^+ + X$
μ^-
X
Relative Probability
E_{obs}/E
4.0
3.5
3.0
2.5
2.0
1.5
1.0
0.5
0
0.2
0.4
0.6
0.8
1.0

Fig. 3(b)

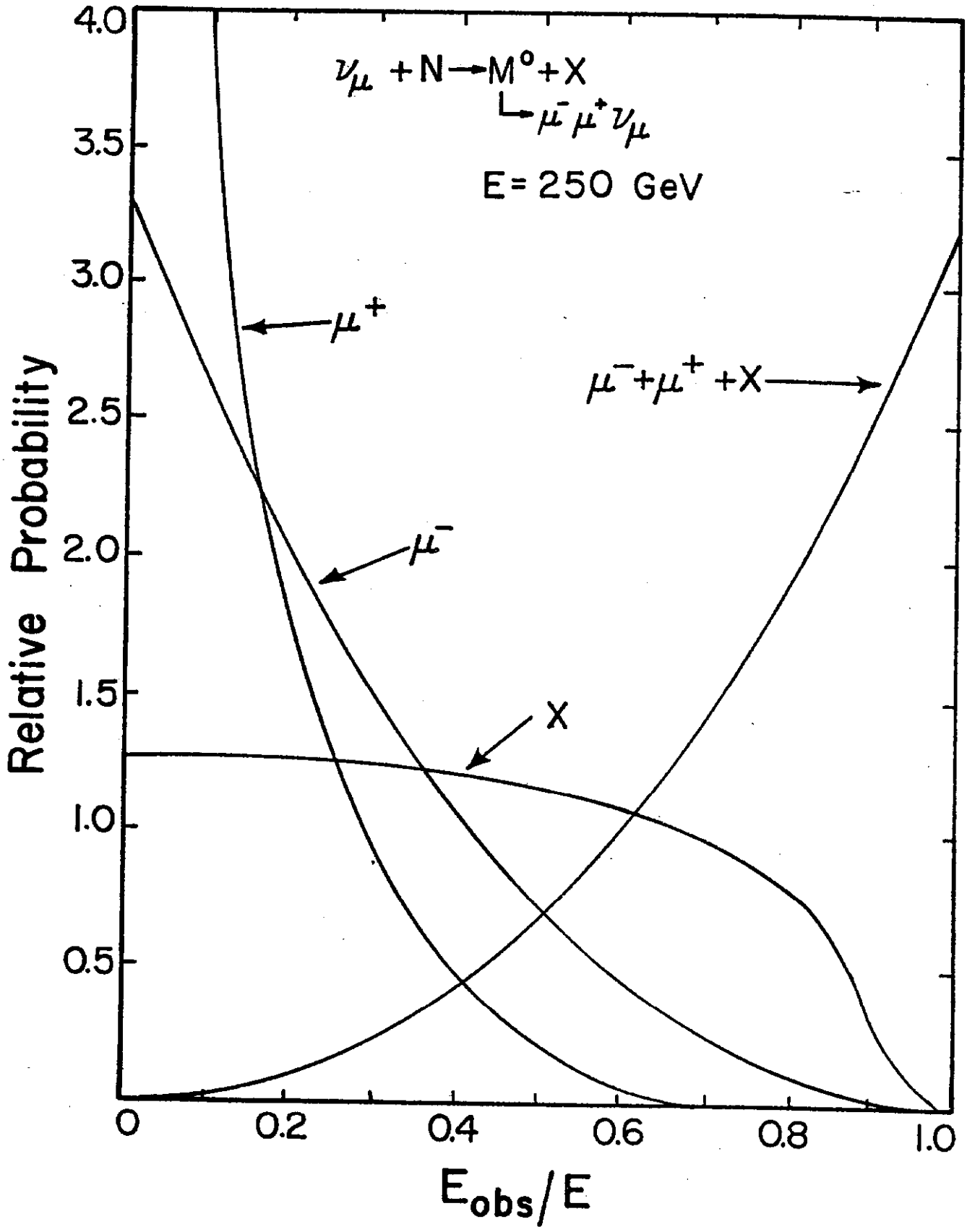
$\nu_\mu + N \rightarrow M^0 + X$
$\hookrightarrow \mu^- \mu^+ \nu_\mu$
E = 250 GeV
μ^+
$\mu^- + \mu^+ + X$
μ^-
X
Relative Probability
4.0
3.5
3.0
2.5
2.0
1.5
1.0
0.5
0
0.2
0.4
0.6
0.8
1.0
E_{obs}/E

Fig. 3(c)

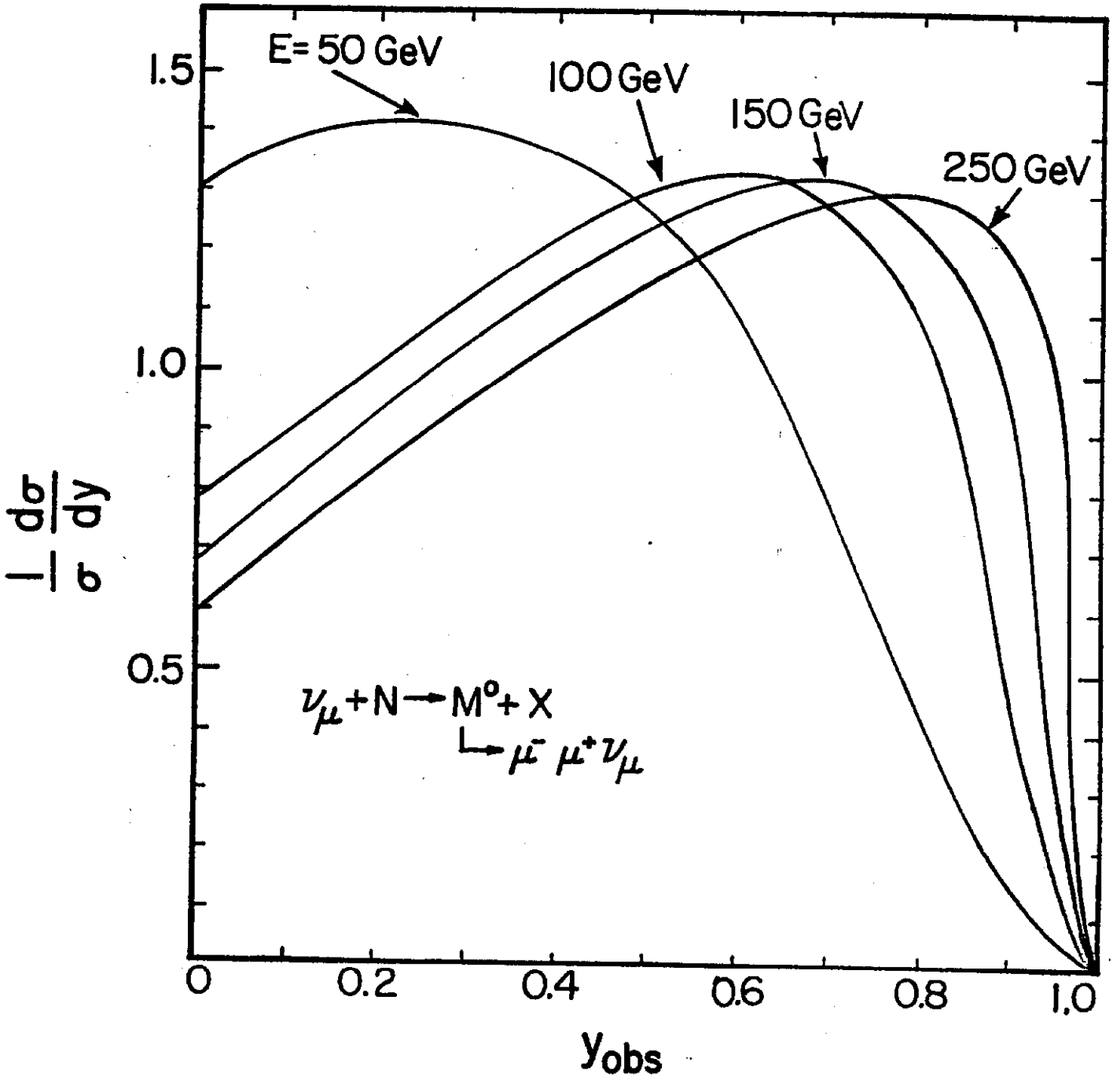
E= 50 GeV
100 GeV
150 GeV
250 GeV
1.5
1.0
0.5
0
0.2
0.4
0.6
0.8
1.0
$\frac{1}{\sigma}\frac{d\sigma}{dy}$
y_{obs}
$\nu_\mu + N \rightarrow M^o + X$
$\hookrightarrow \mu^- \mu^+ \nu_\mu$

Fig. 4

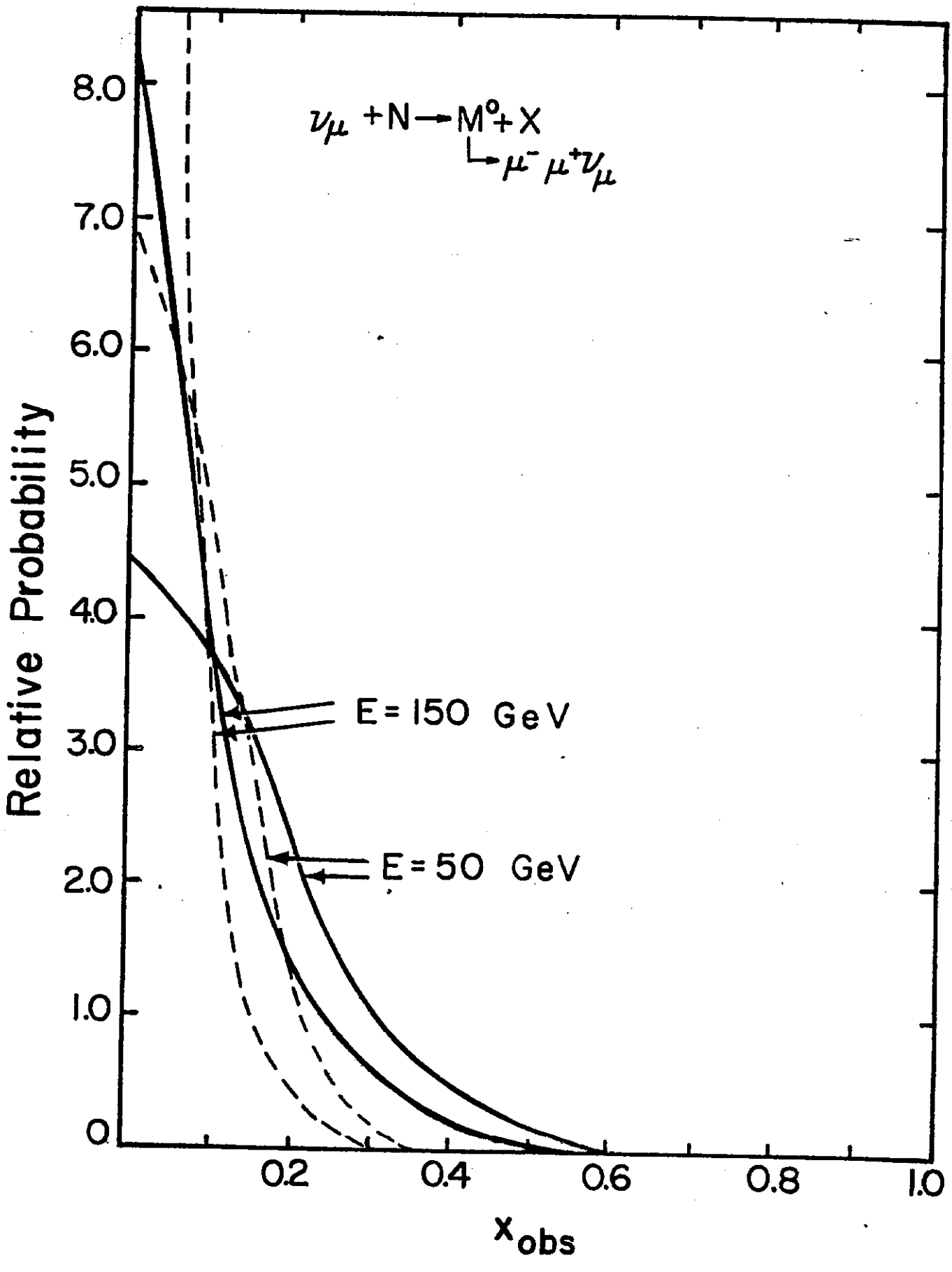
$\nu_\mu + N \rightarrow M^0 + X$
$\hookrightarrow \mu^- \mu^+ \nu_\mu$
E = 150 GeV
E = 50 GeV
Relative Probability
x_{obs}
8.0
7.0
6.0
5.0
4.0
3.0
2.0
1.0
0
0.2
0.4
0.6
0.8
1.0

Fig. 5

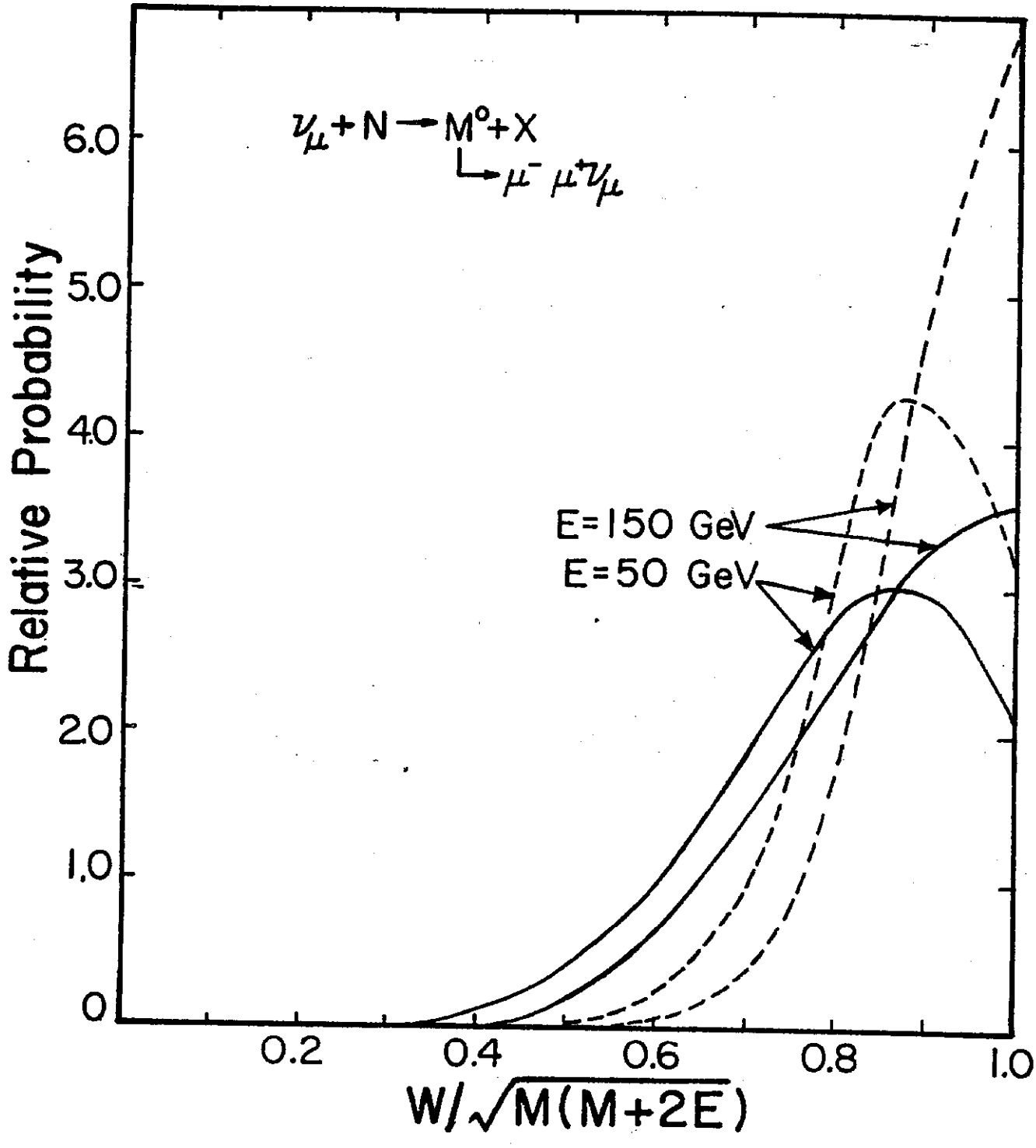
$\nu_\mu + N \rightarrow M^0 + X$
$\hookrightarrow \mu^- \mu^+ \nu_\mu$
Relative Probability
6.0
5.0
4.0
3.0
2.0
1.0
0
E=150 GeV
E=50 GeV
0.2
0.4
0.6
0.8
1.0
$W/\sqrt{M(M+2E)}$

Fig. 6

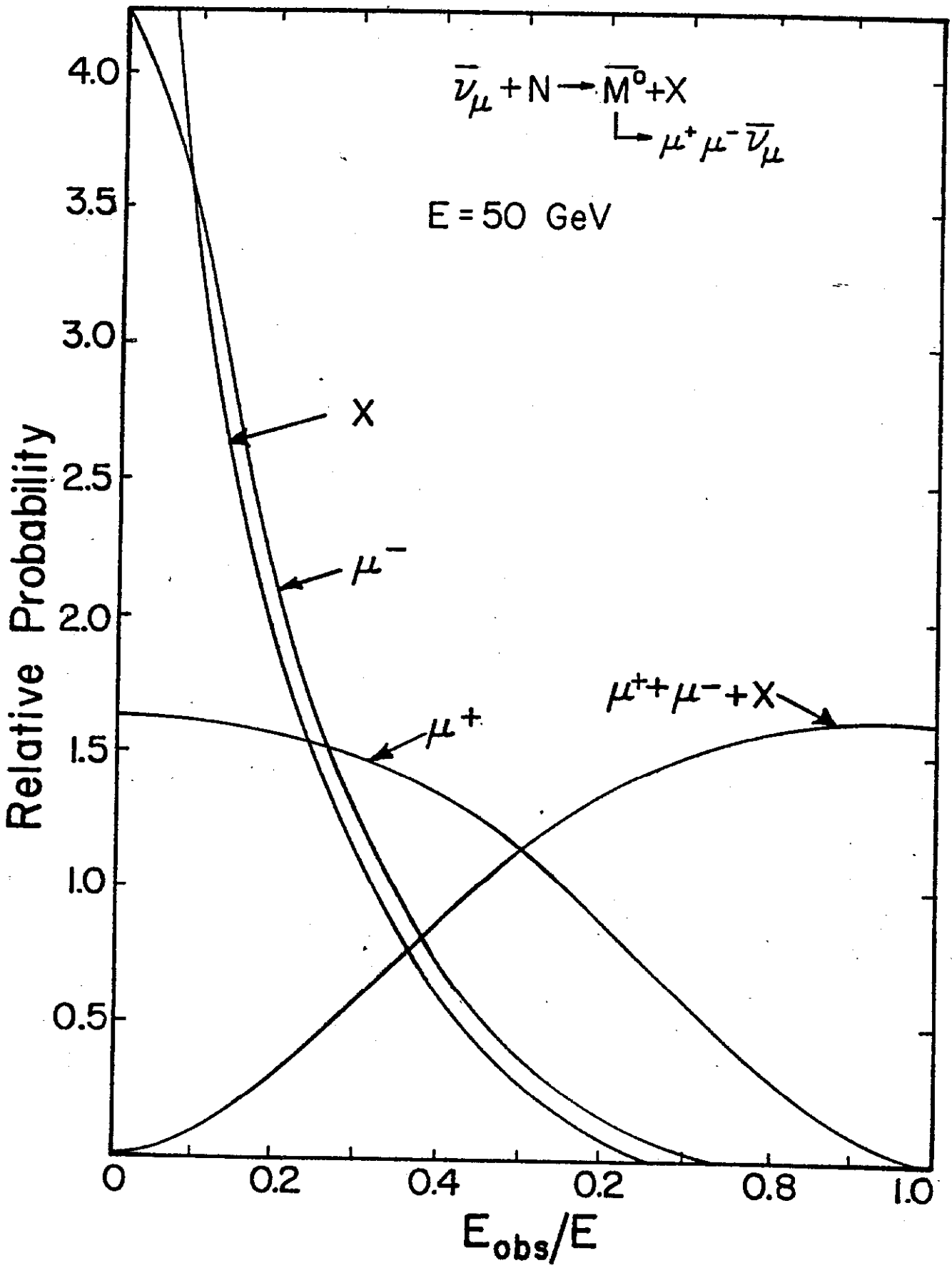
$\bar{\nu}_\mu + N \rightarrow \bar{M}^0 + X$
$\hookrightarrow \mu^+ \mu^- \bar{\nu}_\mu$
E = 50 GeV
X
μ^-
μ^+
$\mu^+ + \mu^- + X$
Relative Probability
4.0
3.5
3.0
2.5
2.0
1.5
1.0
0.5
0
0.2
0.4
0.2
0.8
1.0
E_{obs}/E

Fig. 7(a)

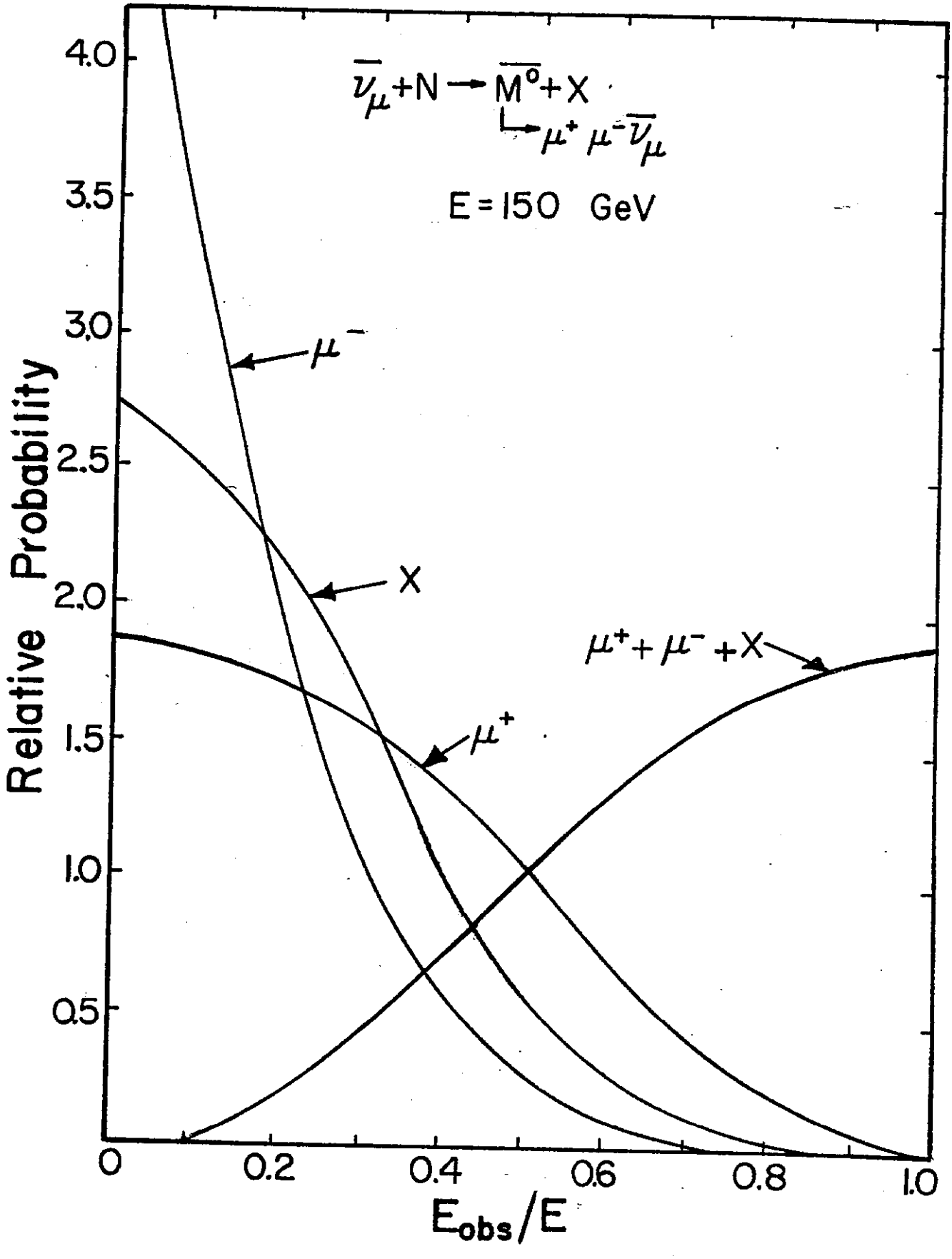
$\bar{\nu}_\mu + N \rightarrow \bar{M}^0 + X$
$\hookrightarrow \mu^+ \mu^- \bar{\nu}_\mu$
E = 150 GeV
μ^-
X
$\mu^+ + \mu^- + X$
μ^+
Relative Probability
E_{obs}/E
4.0
3.5
3.0
2.5
2.0
1.5
1.0
0.5
0
0.2
0.4
0.6
0.8
1.0

Fig. 7(b)

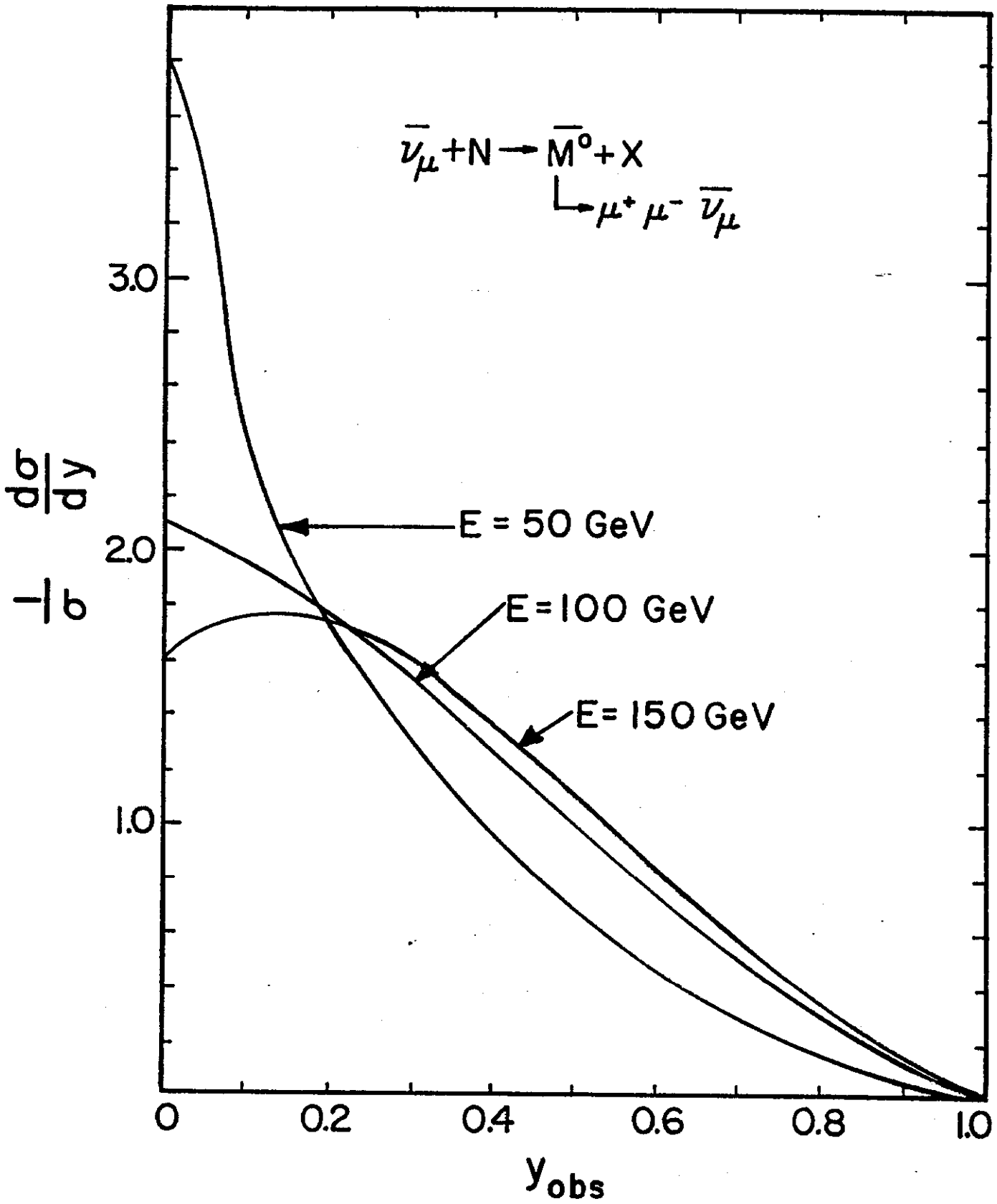
$\bar{\nu}_\mu + N \rightarrow \bar{M}^0 + X$
$\hookrightarrow \mu^+ \mu^- \bar{\nu}_\mu$
E = 50 GeV
E = 100 GeV
E = 150 GeV
$\frac{d\sigma}{dy}$
$\frac{1}{b}$
3.0
2.0
1.0
0
0.2
0.4
0.6
0.8
1.0
y_{obs}

Fig. 8

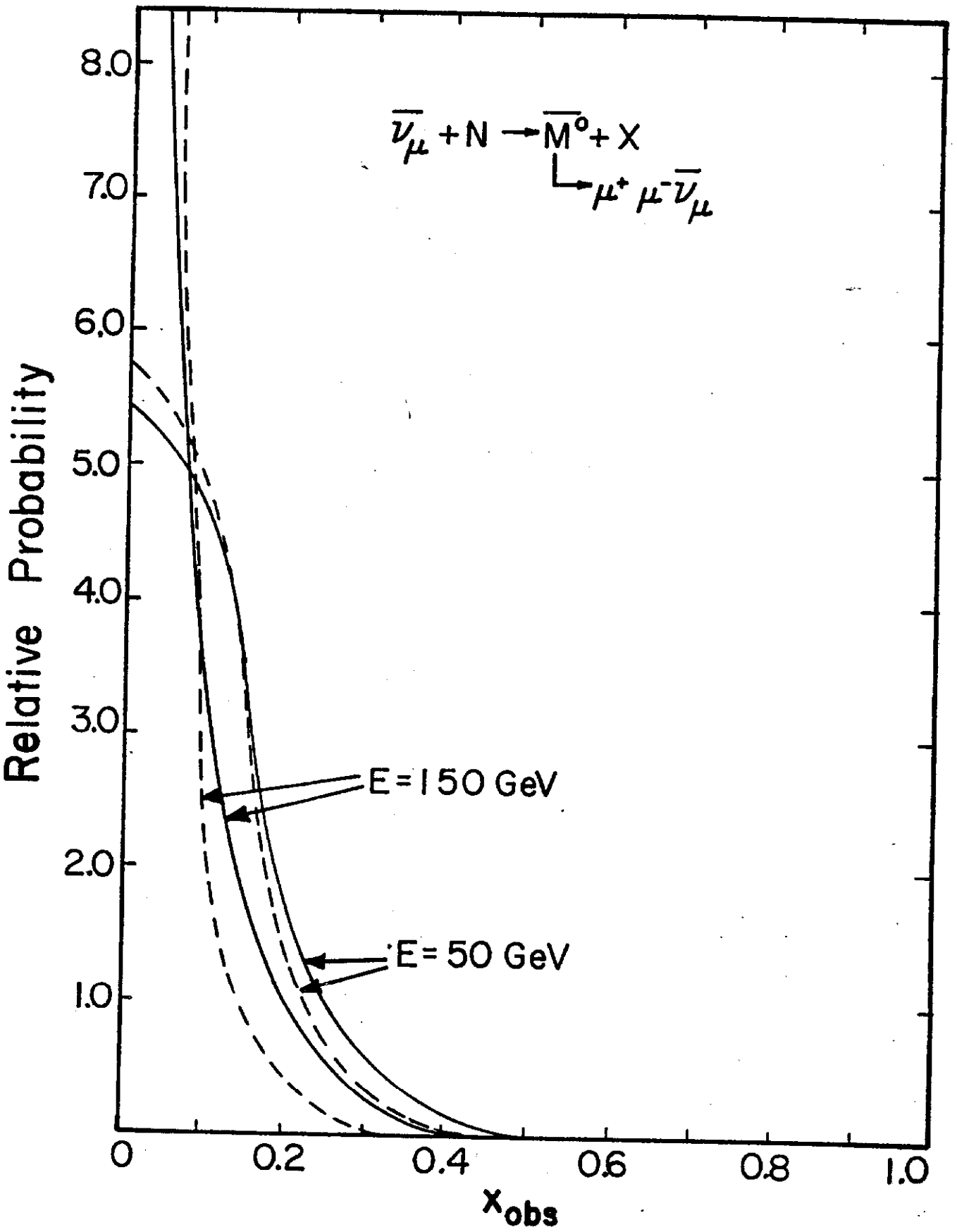
$\bar{\nu}_\mu + N \rightarrow \bar{M}^0 + X$
$\hookrightarrow \mu^+ \mu^- \bar{\nu}_\mu$
Relative Probability
8.0
7.0
6.0
5.0
4.0
3.0
2.0
1.0
0
0.2
0.4
0.6
0.8
1.0
x_{obs}
E = 150 GeV
E = 50 GeV

Fig. 9

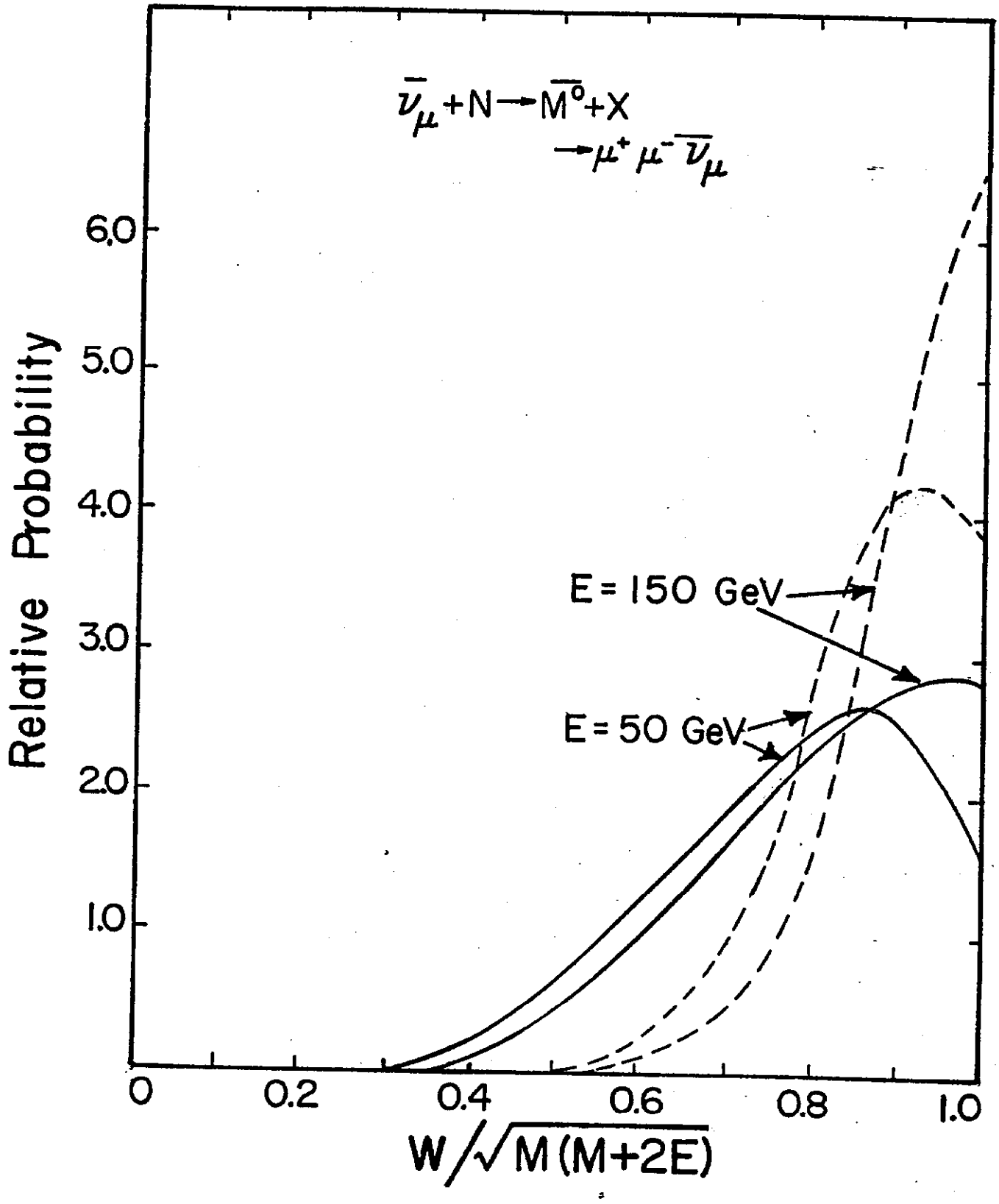
$\bar{\nu}_\mu + N \rightarrow \bar{M}^0 + X$
$\rightarrow \mu^+ \mu^- \bar{\nu}_\mu$
Relative Probability
6.0
5.0
4.0
3.0
2.0
1.0
E = 150 GeV
E = 50 GeV
0
0.2
0.4
0.6
0.8
1.0
$W/\sqrt{M(M+2E)}$

Fig. 10

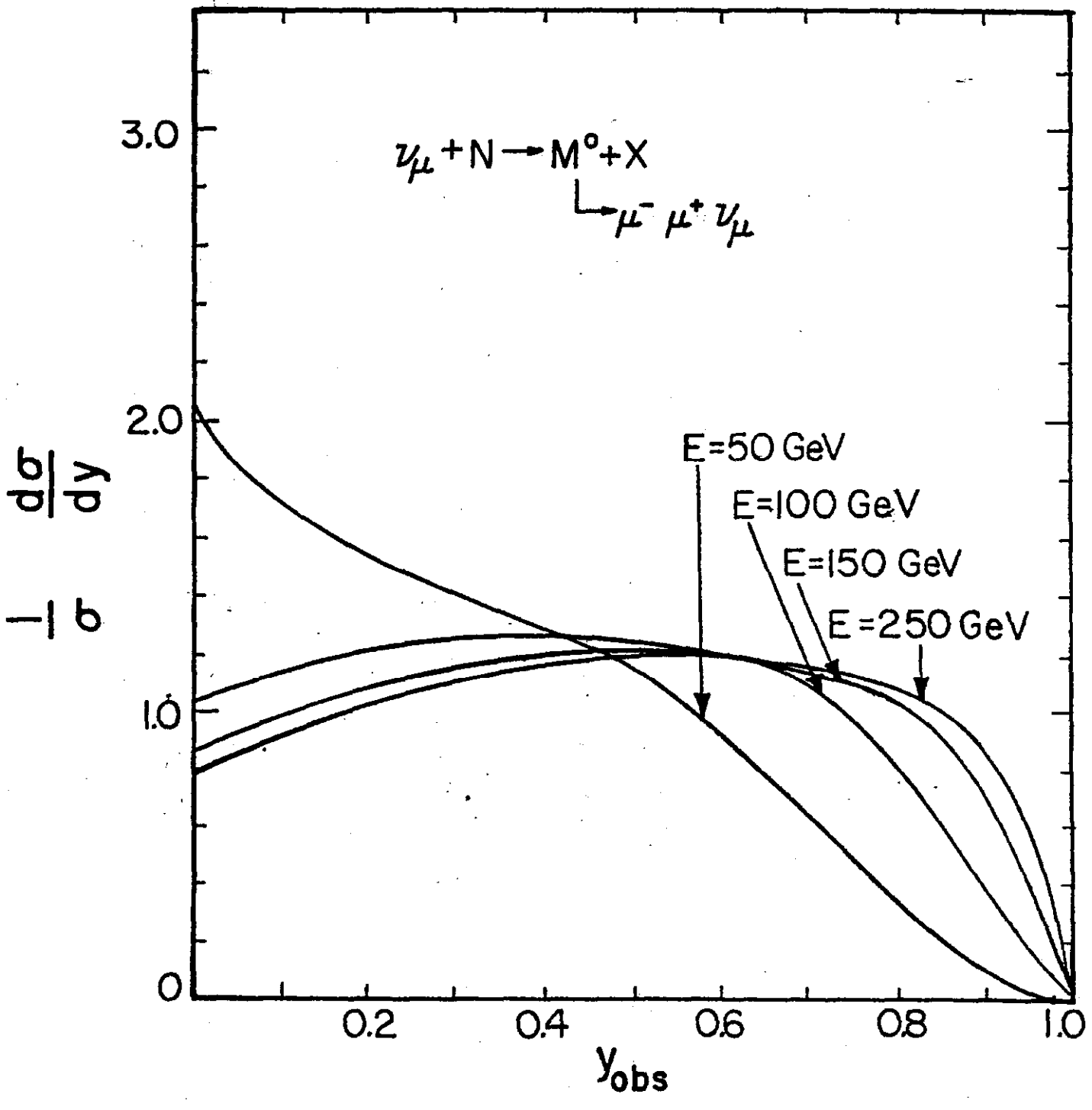
$\nu_\mu + N \rightarrow M^0 + X$
$\hookrightarrow \mu^- \mu^+ \nu_\mu$
E=50 GeV
E=100 GeV
E=150 GeV
E=250 GeV
$\frac{1}{\sigma}\frac{d\sigma}{dy}$
3.0
2.0
1.0
0
0.2
0.4
0.6
0.8
1.0
y_{obs}

Fig. 11

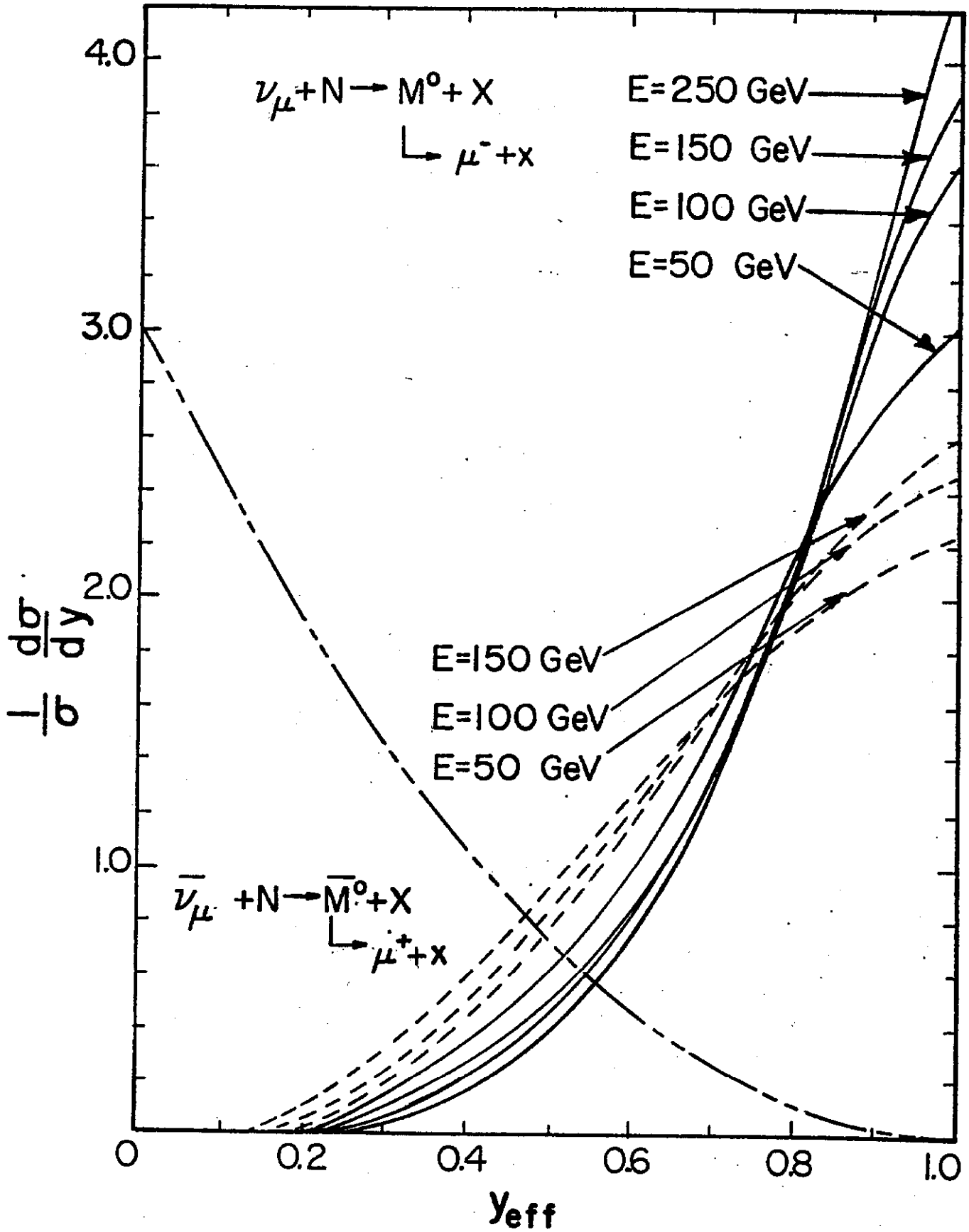
4.0
3.0
2.0
1.0
0
0.2
0.4
0.6
0.8
1.0
$\nu_\mu + N \rightarrow M^0 + X$
$\hookrightarrow \mu^- + x$
E=250 GeV
E=150 GeV
E=100 GeV
E=50 GeV
E=150 GeV
E=100 GeV
E=50 GeV
$\bar{\nu}_\mu + N \rightarrow \bar{M}^0 + X$
$\hookrightarrow \mu^+ + x$
$\frac{d\sigma}{dy}$ — b
y_{eff}

Fig. 12

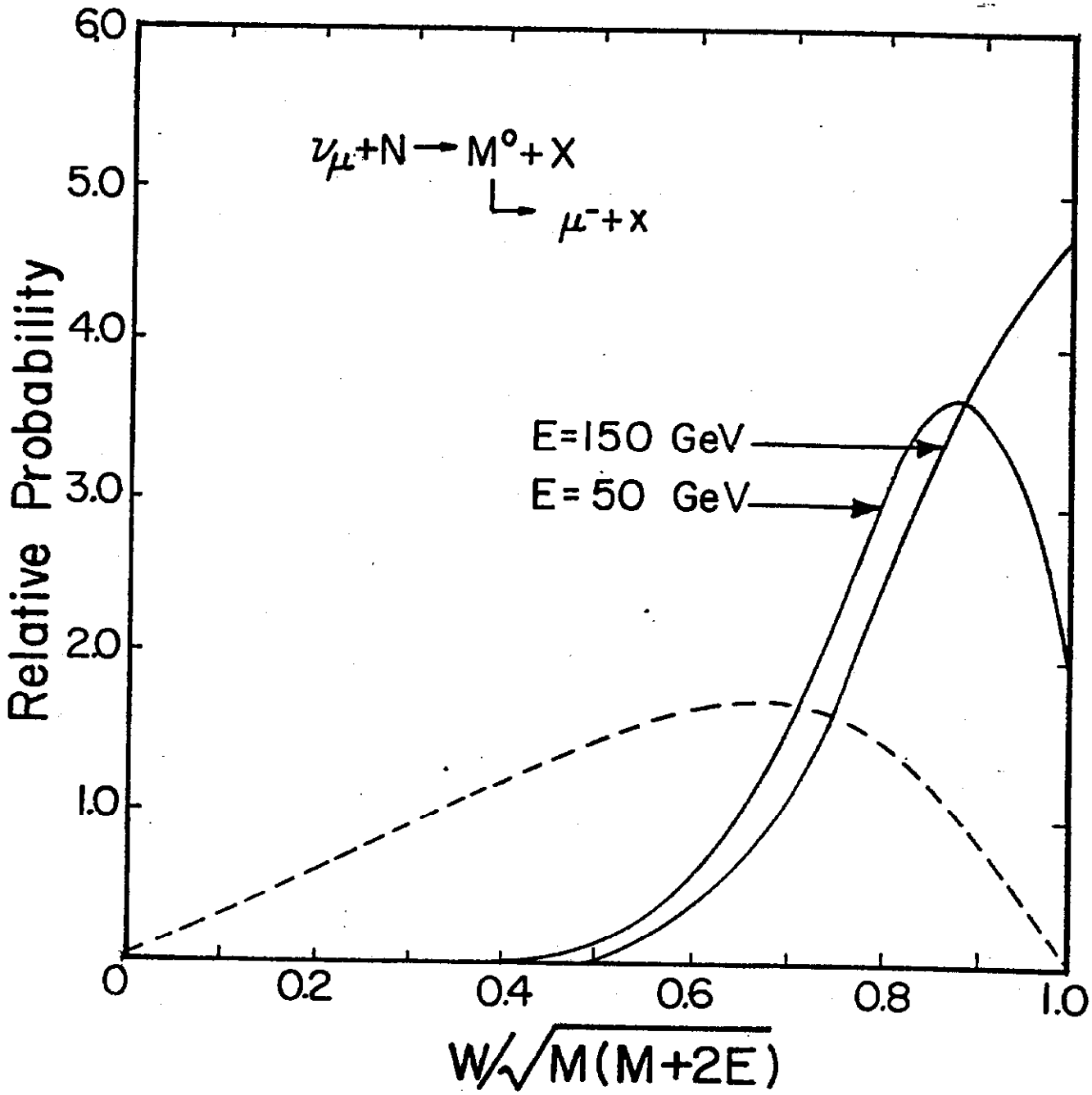
6.0
5.0
4.0
3.0
2.0
1.0
0
0.2
0.4
0.6
0.8
1.0
Relative Probability
$\nu_\mu + N \rightarrow M^\circ + X$
$\hookrightarrow \mu^- + x$
E=150 GeV
E= 50 GeV
$W/\sqrt{M(M+2E)}$

Fig. 13

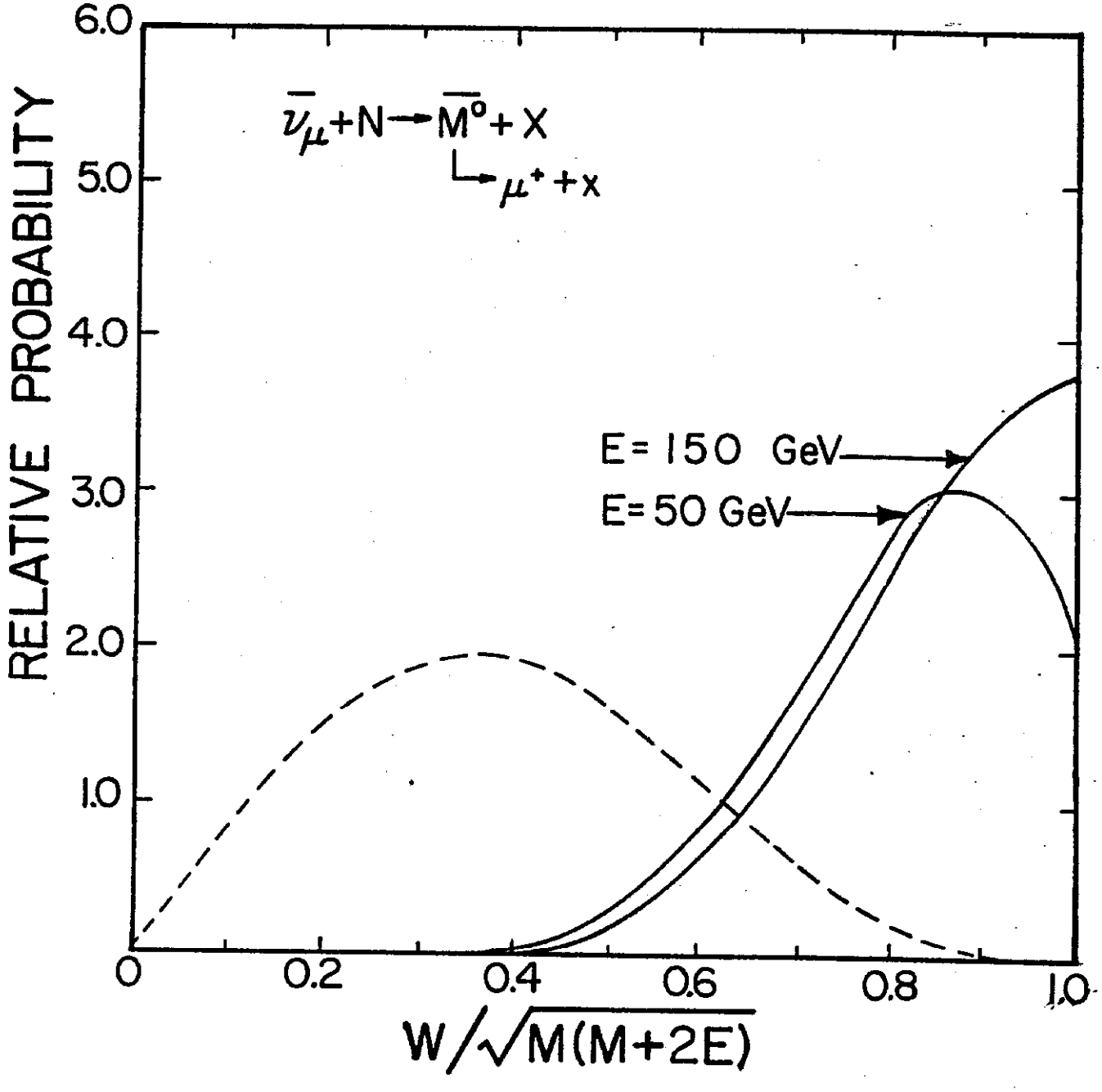
RELATIVE PROBABILITY
6.0
5.0
4.0
3.0
2.0
1.0
0
0.2
0.4
0.6
0.8
1.0
$\bar{\nu}_\mu + N \rightarrow \bar{M}^0 + X$
$\hookrightarrow \mu^+ + x$
E = 150 GeV
E = 50 GeV
$W/\sqrt{M(M+2E)}$

Fig. 14

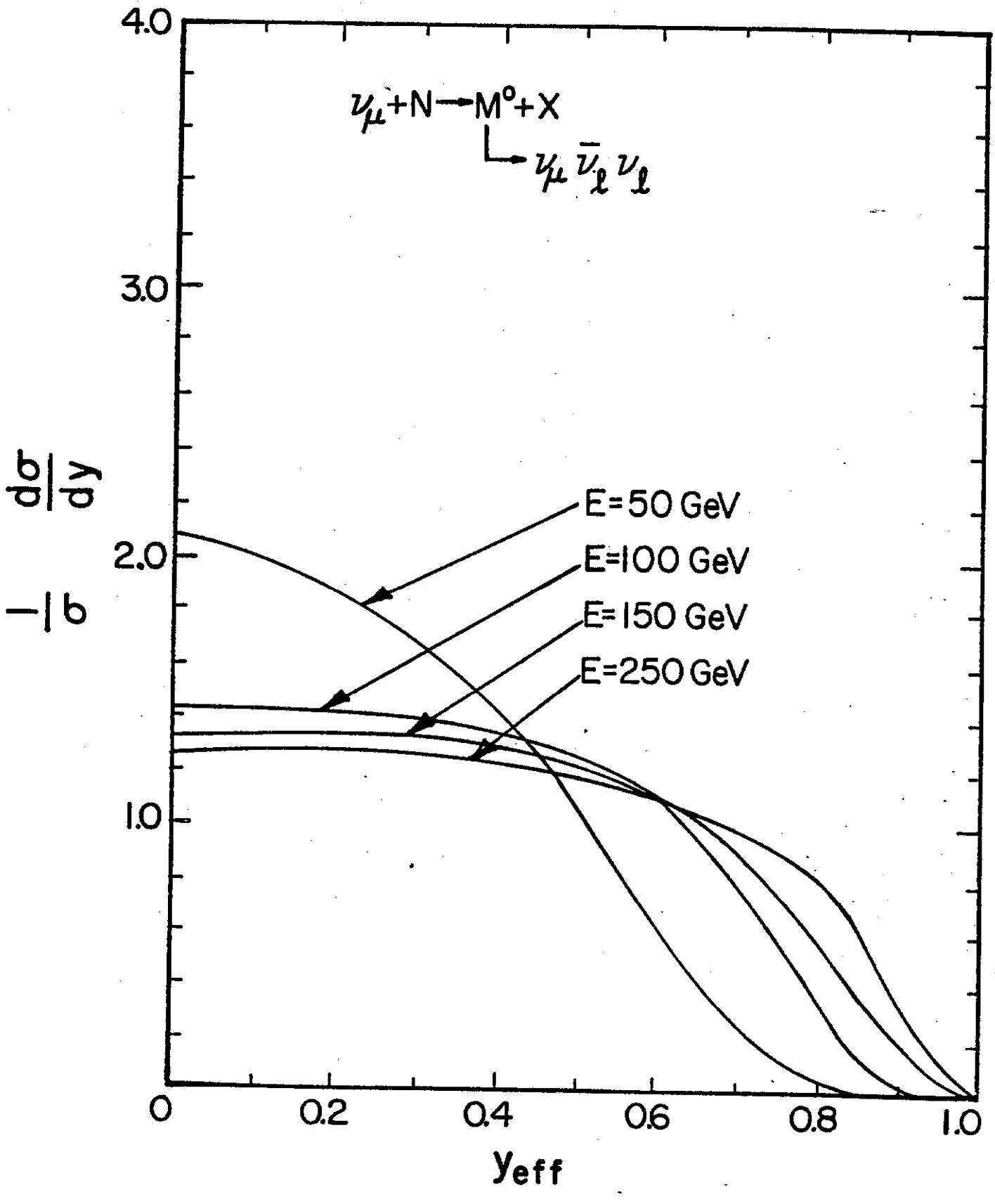
4.0
3.0
2.0
1.0
0
0.2
0.4
0.6
0.8
1.0
$\nu_\mu + N \rightarrow M^0 + X$
$\hookrightarrow \nu_\mu \bar{\nu}_\ell \nu_\ell$
E=50 GeV
E=100 GeV
E=150 GeV
E=250 GeV
$\frac{d\sigma}{dy}$
$-|b$
y_{eff}

Fig. 15

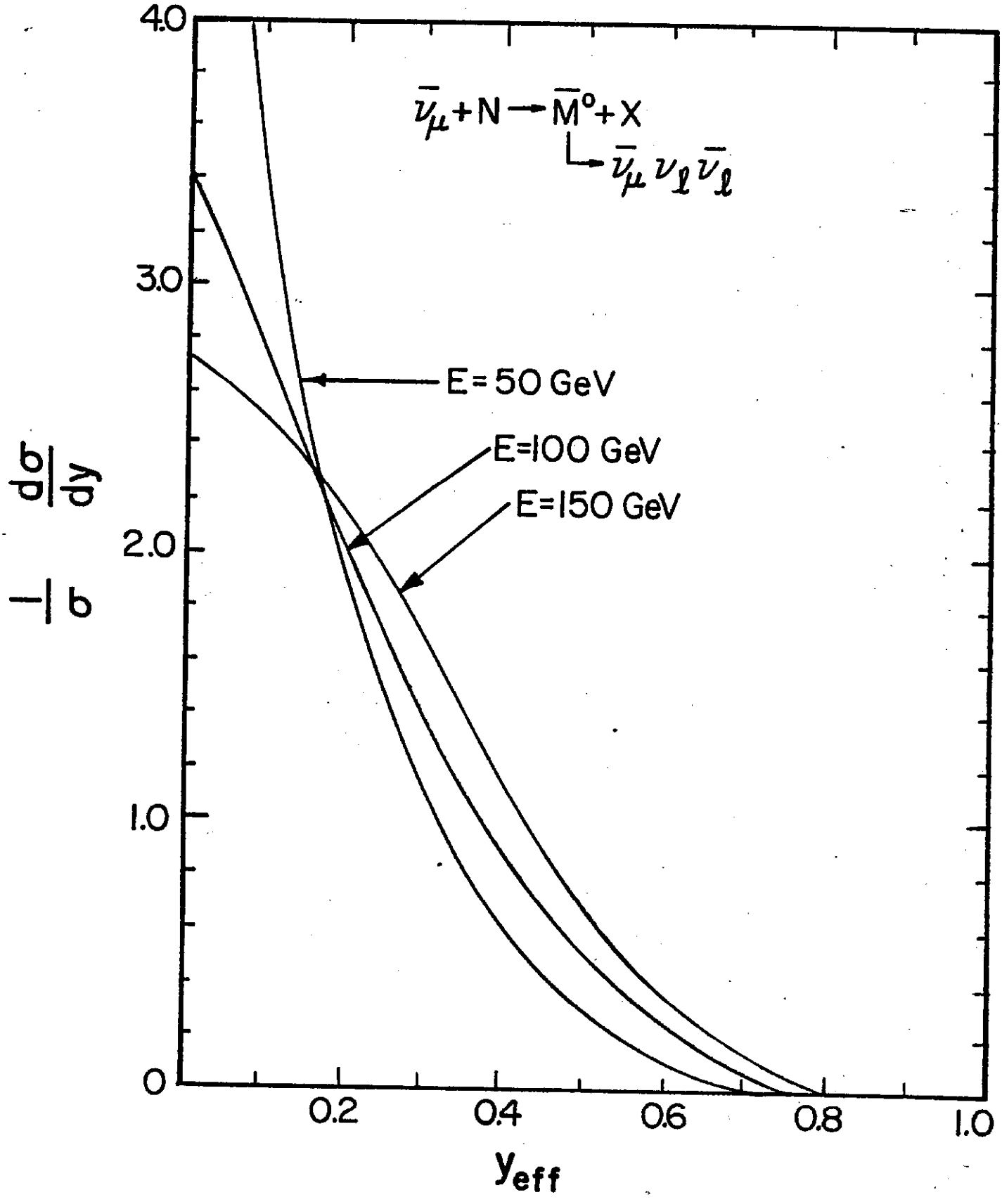
4.0
3.0
2.0
1.0
0
0.2
0.4
0.6
0.8
1.0
$\bar{\nu}_\mu + N \rightarrow \bar{M}^0 + X$
$\hookrightarrow \bar{\nu}_\mu \nu_\ell \bar{\nu}_\ell$
E = 50 GeV
E=100 GeV
E=150 GeV
$\frac{1}{\sigma}\frac{d\sigma}{dy}$
y_{eff}

Fig. 16